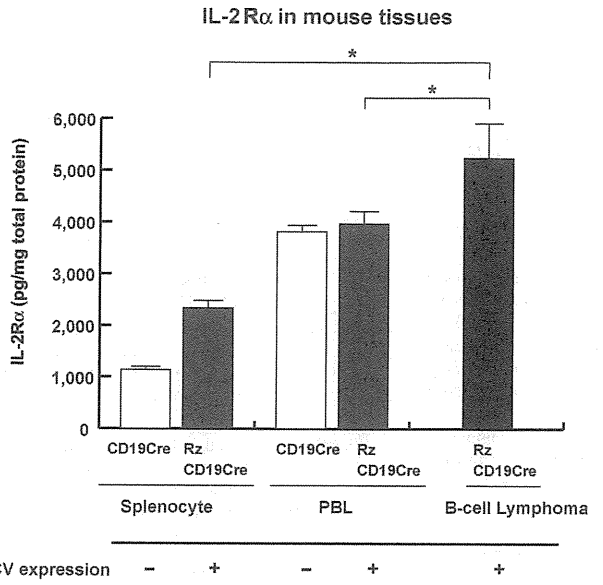

Figure 5. Levels of IL-2Rα in transgenic and control mice lacking or harboring B-cell lymphomas. The expression level of IL-2Rα in splenocytes and PBLs from CD19Cre and RzCD19Cre mice and in B-cell lymphomas from RzCD19Cre mice was measured by ELISA. IL-2Rα levels per total protein are indicated (picograms per milligram). Data from quadruplicate samples are shown as the mean ± SD (*$P < .05$).

RzCD19Cre mice with B-cell lymphomas, 72.2 ± 60.5 IU/L; normal controls, 55.2 ± 23.0 IU/L and ALT: RzCD19Cre mice with B-cell lymphomas, 14.2 ± 3.1 IU/L; normal controls, 11.5 ± 3.0 IU/L).

Finally, we examined the level of sIL-2Rα in the sera of the RzCD19Cre mice with B-cell lymphomas; sIL-2Rα is generated by proteolytic cleavage of IL-2Rα (CD25) residing on the surface of activated T and natural killer cells, monocytes, and certain tumor cells.[24,32] The average sIL-2Rα level in the RzCD19Cre mice with B-cell lymphomas (830.3 ± 533.0 pg/mL) was significantly higher than that in the tumor-free control groups, including the RzCD19Cre, Rz, CD19Cre and WT mice (499.9 ± 110.2 pg/mL; $P < .0057$; Figure 4C). The average sIL-2Rα levels in other tumor-containing groups (430.46 ± 141.15 pg/mL) were not significantly different from those in the tumor-free control groups ($P > .05$; Figure 4C). Moreover, all RzCD19Cre mice with a relatively high level of sIL-2Rα (> 1000 pg/mL) presented with B-cell lymphomas (Figure 4C).

We also examined the level of sIL-2Rα in MxCre/CN2-29 mice and observed a significant increase in sIL-2Rα in mice that expressed HCV and that had B-cell lymphomas compared with tumor-free control (CN2-29) mice (Figure 4D).

Expression of IL-2Rα in B-cell lymphomas of the RzCD19Cre mice

To examine whether sIL-2Rα was derived from lymphoma tissues, we quantified IL-2Rα concentrations in splenocytes, PBLs and B-cell lymphoma tissues (Figure 5). The concentration of IL-2Rα was significantly higher in splenocytes from RzCD19Cre mice compared with those from CD19Cre mice; the concentration was even higher in B-cell lymphoma tissues than in splenocytes from RzCD19Cre mice (Figure 5). These results strongly suggest that B-cell lymphomas directly contribute to the elevated serum concentrations of sIL-2Rα in RzCD19Cre mice.

Discussion

We have established HCV transgenic mice that have a high incidence of spontaneous B-cell lymphomas. In this animal model, the HCV transgene is expressed during the embryonic stage, and these RzCD19Cre mice are expected to be immunotolerant to the HCV transgene product. Thus, the results from this study reveal the potential for the HCV gene to induce B-cell lymphomas without inducing host immune responses against the HCV gene product. A retrospective study indicated that viral elimination reduced the incidence of malignant lymphoma in patients infected with HCV.[33] The results in our study may be consistent with this retrospective observation, indicating the significance of the direct effect of HCV infection on B-cell lymphoma development. Another HCV transgenic mouse strain (MxCre/CN2-29) showed the similarly high incidence of B-cell lymphoma, which strongly supported that development of B-cell lymphomas occurred by the expression of HCV transgene.

Recent findings have revealed the significance of B lymphocytes in HCV infection of liver-derived hepatoma cells.[34] In 4.2% of the RzCD19Cre mice, CD45R-positive intrahepatic lymphomas were identified, and infiltration of B cells into the hepatocytes was frequently observed (data not shown). These phenomena suggest that HCV could modify the in vivo tropism of B cells. The RzCD19Cre mouse is a powerful model system to address these mechanisms in vivo.

As a circulating membrane receptor, sIL-2Rα is localized in lymphoid cells and some other types of cancer cells and is highly expressed in several cancers[35-40] and autoimmune diseases.[41] Recent findings indicate a link between sIL-2Rα levels and hepatocellular carcinoma in Egyptian patients.[42] Appearing on the surface of leukemic cells derived from B and pre-B lymphocytes and other leukemic cells, IL-2Rα is one of the subunits of the IL-2 receptor, which is composed of an α chain (CD25), a β chain (CD122), and a γ chain (CD132).[43] IL-2R ectodomains are thought to be proteolytically cleaved from the cell surface[34,44,45] instead of produced as a result of posttranscriptional splicing.[24] In RzCD19Cre splenocytes, the level of IL-2Rα was higher than that in splenocytes from CD19Cre mice; however, serum concentrations of sIL-2Rα in RzCD19Cre mice without B-cell lymphomas did not show significant differences compared with other control groups (Rz, CD19Cre, and WT). These results indicate the possibility that HCV may increase IL-2Rα expression on B-cells; proteolytic cleavage of IL-2Rα was increased after B-cell lymphoma development in the RzCD19Cre mouse. The detailed mechanism that induces IL-2Rα as a result of HCV expression is still unclear at present, but we have found previously that the HCV core protein induces IL-10 expression in mouse splenocytes.[14] IL-10 up-regulates the expression of IL-2Rα (Tac/CD25) on normal and leukemic B lymphocytes,[46] and therefore, through IL-10, the HCV core protein might induce IL-2Rα in B cells of the RzCD19Cre mouse.

In conclusion, this study established an animal model that will likely provide critical information for the elucidation of molecular mechanism(s) underlying the spontaneous development of B-cell non-Hodgkin lymphoma after HCV infection. This knowledge should lead to therapeutic strategies to prevent the onset and/or progression of B-cell lymphomas.

Acknowledgments

We thank Dr T. Ito for assistance with pathology characterization and Dr T. Munakata for valuable comments.

This work was supported by grants from the Ministry of Health and Welfare of Japan and the Cooperative Research Project on Clinical and Epidemiologic Studies of Emerging and Re-emerging Infectious Diseases.

Authorship

Contribution: K.T.-K. conceived of the project; K.K., M.K., and K.T.-K. designed the studies; Y.K., S.S., M. Saito, K.T., M. Satoh, M.T., and K.T.-K. performed experiments and analyses; N.S. and Y.H. provided scientific advice; and K.T.-K. wrote the manuscript.

Conflict-of-interest disclosure: The authors declare no competing financial interests.

Correspondence: Kyoko Tsukiyama-Kohara, Department of Experimental Phylaxiology, Faculty of Life Sciences, Kumamoto University, Kumamoto 860-8556, Japan; e-mail: kkohara@kumamoto-u.ac.jp.

References

1. Ferri C, Monti M, La Civita L, et al. Infection of peripheral blood mononuclear cells by hepatitis C virus in mixed cryoglobulinemia. *Blood.* 1993; 82(12):3701-3704.
2. Saito I, Miyamura T, Ohbayashi A, et al. Hepatitis C virus infection is associated with the development of hepatocellular carcinoma. *Proc Natl Acad Sci U S A.* 1990;87(17):6547-6549.
3. Simonetti RG, Camma C, Fiorello F, et al. Hepatitis C virus infection as a risk factor for hepatocellular carcinoma in patients with cirrhosis. A case-control study. *Ann Intern Med.* 1992;116(2):97-102.
4. Silvestri F, Pipan C, Barillari G, et al. Prevalence of hepatitis C virus infection in patients with lymphoproliferative disorders. *Blood.* 1996;87(10): 4296-4301.
5. Ascoli V, Lo Coco F, Artini M, Levrero M, Martelli M, Negro F. Extranodal lymphomas associated with hepatitis C virus infection. *Am J Clin Pathol.* 1998;109(5):600-609.
6. Mele A, Pulsoni A, Bianco E, et al. Hepatitis C virus and B-cell non-Hodgkin lymphomas: an Italian multicenter case-control study. *Blood.* 2003; 102(3):996-999.
7. Dammacco F, Sansonno D, Piccoli C, Racanelli V, D'Amore FP, Lauletta G. The lymphoid system in hepatitis C virus infection: autoimmunity, mixed cryoglobulinemia, and overt B-cell malignancy. *Semin Liver Dis.* 2000;20(2):143-157.
8. Gisbert JP, Garcia-Buey L, Pajares JM, Moreno-Otero R. Prevalence of hepatitis C virus infection in B-cell non-Hodgkin's lymphoma: systematic review and meta-analysis. *Gastroenterology.* 2003;125(6):1723-1732.
9. Negri E, Little D, Boiocchi M, La Vecchia C, Franceschi S. B-cell non-Hodgkin's lymphoma and hepatitis C virus infection: a systematic review. *Int J Cancer.* 2004;111(1):1-8.
10. Pileri P, Uematsu Y, Campagnoli S, et al. Binding of hepatitis C virus to CD81. *Science.* 1998; 282(5390):938-941.
11. Rosa D, Saletti G, De Gregorio E, et al. Activation of naive B lymphocytes via CD81, a pathogenetic mechanism for hepatitis C virus-associated B lymphocyte disorders. *Proc Natl Acad Sci U S A.* 2005;102(51):18544-18549.
12. Wakita T, Taya C, Katsume A, et al. Efficient conditional transgene expression in hepatitis C virus cDNA transgenic mice mediated by the Cre/loxP system. *J Biol Chem.* 1998;273(15):9001-9006.
13. Machida K, Tsukiyama-Kohara K, Seike E, et al. Inhibition of cytochrome c release in Fas-mediated signaling pathway in transgenic mice induced to express hepatitis C viral proteins. *J Biol Chem.* 2001;276(15):12140-12146.
14. Machida K, Tsukiyama-Kohara K, Sekiguch S, et al. Hepatitis C virus and disrupted interferon signaling promote lymphoproliferation via type II CD95 and interleukins. *Gastroenterology.* 2009; 137(1):285-296,296 e281-211.
15. Lerat H, Rumin S, Habersetzer F, et al. In vivo tropism of hepatitis C virus genomic sequences in hematopoietic cells: influence of viral load, viral genotype, and cell phenotype. *Blood.* 1998; 91(10):3841-3849.
16. Karavattathayyil SJ, Kalkeri G, Liu HJ, et al. Detection of hepatitis C virus RNA sequences in B-cell non-Hodgkin lymphoma. *Am J Clin Pathol.* 2000;113(3):391-398.
17. Rickert RC, Roes J, Rajewsky K. B lymphocyte-specific, Cre-mediated mutagenesis in mice. *Nucleic Acids Res.* 1997;25(6):1317-1318.
18. Tanaka T, Lau JY, Mizokami M, et al. Simple fluorescent enzyme immunoassay for detection and quantification of hepatitis C viremia. *J Hepatol.* 1995;23(6):742-745.
19. Tsukiyama-Kohara K, Tone S, Maruyama I, et al. Activation of the CKI-CDK-Rb-E2F pathway in full genome hepatitis C virus-expressing cells. *J Biol Chem.* 2004;279(15):14531-14541.
20. Nishimura T, Kohara M, Izumi K, et al. Hepatitis C virus impairs p53 via persistent overexpression of 3beta-hydroxysterol Delta24-reductase. *J Biol Chem.* 2009;284(52):36442-36452.
21. Tsukiyama-Kohara K, Poulin F, Kohara M, et al. Adipose tissue reduction in mice lacking the translational inhibitor 4E-BP1. *Nat Med.* 2001; 7(10):1128-1132.
22. Fujimura S, Xing Y, Takeya M, et al. Increased expression of germinal center-associated nuclear protein RNA-primase is associated with lymphomagenesis. *Cancer Res.* 2005;65(13):5925-5934.
23. Miyazaki T, Kato I, Takeshita S, Karasuyama H, Kudo A. Lambda5 is required for rearrangement of the Ig kappa light chain gene in pro-B cell lines. *Int Immunol.* 1999;11(8):1195-1202.
24. Rubin LA, Galli F, Greene WC, Nelson DL, Jay G. The molecular basis for the generation of the human soluble interleukin 2 receptor. *Cytokine.* 1990;2(5):330-336.
25. Tsukiyama-Kohara K, Iizuka N, Kohara M, Nomoto A. Internal ribosome entry site within hepatitis C virus RNA. *J Virol.* 1992;66(3):1476-1483.
26. Jaffe ES, Harris NL, Stein H, Isaacson PG. Classification of lymphoid neoplasms: the microscope as a tool for disease discovery. *Blood.* 2008; 112(12):4384-4399.
27. el-Din HM, Attia MA, Hamza MR, Khaled HM, Thoraya MA, Eisa SA. Hepatitis C Virus and related changes in immunologic parameters in non Hodgkin's lymphoma patients. *Egypt J Immunol.* 2004;11(1):55-64.
28. Feldmann G, Nischalke HD, Nattermann J, et al. Induction of interleukin-6 by hepatitis C virus core protein in hepatitis C-associated mixed cryoglobulinemia and B-cell non-Hodgkin's lymphoma. *Clin Cancer Res.* 2006;12(15):4491-4498.
29. Mizuochi T, Ito M, Takai K, Yamaguchi K. Differential susceptibility of peripheral blood CD5+ and CD5− B cells to apoptosis in chronic hepatitis C patients. *Biochem Biophys Res Commun.* 2009; 389(3):512-515.
30. Bansal AS, Bruce J, Hogan PG, Prichard P, Powell EE. Serum soluble CD23 but not IL8, IL10, GM-CSF, or IFN-gamma is elevated in patients with hepatitis C infection. *Clin Immunol Immunopathol.* 1997;84(2):139-144.
31. Barrett L, Gallant M, Howley C, et al. Enhanced IL-10 production in response to hepatitis C virus proteins by peripheral blood mononuclear cells from human immunodeficiency virus-monoinfected individuals. *BMC Immunol.* 2008;9:28.
32. Rubin LA, Kurman CC, Fritz ME, et al. Soluble interleukin 2 receptors are released from activated human lymphoid cells in vitro. *J Immunol.* 1985;135(5):3172-3177.
33. Kawamura Y, Ikeda K, Arase Y, et al. Viral elimination reduces incidence of malignant lymphoma in patients with hepatitis C. *Am J Med.* 2007; 120(12):1034-1041.
34. Stamataki Z, Shannon-Lowe C, Shaw J, et al. Hepatitis C virus association with peripheral blood B lymphocytes potentiates viral infection of liver-derived hepatoma cells. *Blood.* 2009;113(3): 585-593.
35. Wasik MA, Sioutos N, Tuttle M, Butmarc JR, Kaplan WD, Kadin ME. Constitutive secretion of soluble interleukin-2 receptor by human T cell lymphoma xenografted into SCID mice. Correlation of tumor volume with concentration of tumor-derived soluble interleukin-2 receptor in body fluids of the host mice. *Am J Pathol.* 1994;144(5): 1089-1097.
36. Tsai MH, Chiou SH, Chow KC. Effect of platelet activating factor and butyrate on the expression of interleukin-2 receptor alpha in nasopharyngeal carcinoma cells. *Int J Oncol.* 2001;19(5):1049-1055.
37. Yano T, Yoshino I, Yokoyama H, et al. The clinical significance of serum soluble interleukin-2 receptors in lung cancer. *Lung Cancer.* 1996;15(1):79-84.
38. Tesarova P, Kvasnicka J, Umlaufova A, Homolkova H, Jirsa M, Tesar V. Soluble TNF and IL-2 receptors in patients with breast cancer. *Med Sci Monit.* 2000;6(4):661-667.
39. Maccio A, Lai P, Santona MC, Pagliara L, Melis GB, Mantovani G. High serum levels of soluble IL-2 receptor, cytokines, and C reactive protein correlate with impairment of T cell response in patients with advanced epithelial ovarian cancer. *Gynecol Oncol.* 1998;69(3):248-252.
40. Matsumoto T, Furukawa A, Sumiyoshi Y, Akiyama KY, Kanayama HO, Kagawa S. Serum levels of soluble interleukin-2 receptor in renal cell carcinoma. *Urology.* 1998;51(1):145-149.
41. Pountain G, Hazleman B, Cawston TE. Circulating levels of IL-1beta, IL-6 and soluble IL-2 receptor in polymyalgia rheumatica and giant cell arteritis and rheumatoid arthritis. *Br J Rheumatol.* 1998;37(7):797-798.
42. Zekri AR, Alam El-Din HM, Bahnassy AA, et al. Serum levels of soluble Fas, soluble tumor necrosis factor-receptor II, interleukin-2 receptor and interleukin-8 as early predictors of hepatocellular carcinoma in Egyptian patients with hepatitis C virus genotype-4. *Comp Hepatol.* 2010:9(1):1.
43. Sheibani K, Winberg CD, van de Velde S, Blayney DW, Rappaport H. Distribution of lymphocytes with interleukin-2 receptors (TAC antigens) in reactive lymphoproliferative processes, Hodgkin's disease, and non-Hodgkin's lymphomas. An immunohistologic study of 300 cases. *Am J Pathol.* 1987;127(1):27-37.
44. Robb RJ, Rusk CM. High and low affinity receptors for interleukin 2: implications of pronase, phorbol ester, and cell membrane studies upon the basis for differential ligand affinities. *J Immunol.* 1986;137(1):142-149.
45. Sheu BC, Hsu SM, Ho HN, Lien HC, Huang SC, Lin RH. A novel role of metalloproteinase in cancer-mediated immunosuppression. *Cancer Res.* 2001;61(1):237-242.
46. Fluckiger AC, Garrone P, Durand I, Galizzi JP, Banchereau J. Interleukin 10 (IL-10) up-regulates functional high affinity IL-2 receptors on normal and leukemic B lymphocytes. *J Exp Med.* 1993; 178(5):1473-1481.

Baumann S, Dostert A, Novac N, et al. Glucocorticoids inhibit activation-induced cell death (AICD) via direct DNA-dependent repression of the CD95 ligand gene by a glucocorticoid receptor dimer. *Blood.* 2005;106(2):617-625.

On page 620 of the 15 July 2005 issue, the lower panels in Figure 3A, representing 2 different experimental conditions (with and without Dex), and the panels in Figure 3C, representing 2 different experimental conditions (with and without CHX), were duplicated. The corrected Figure 3 is shown.

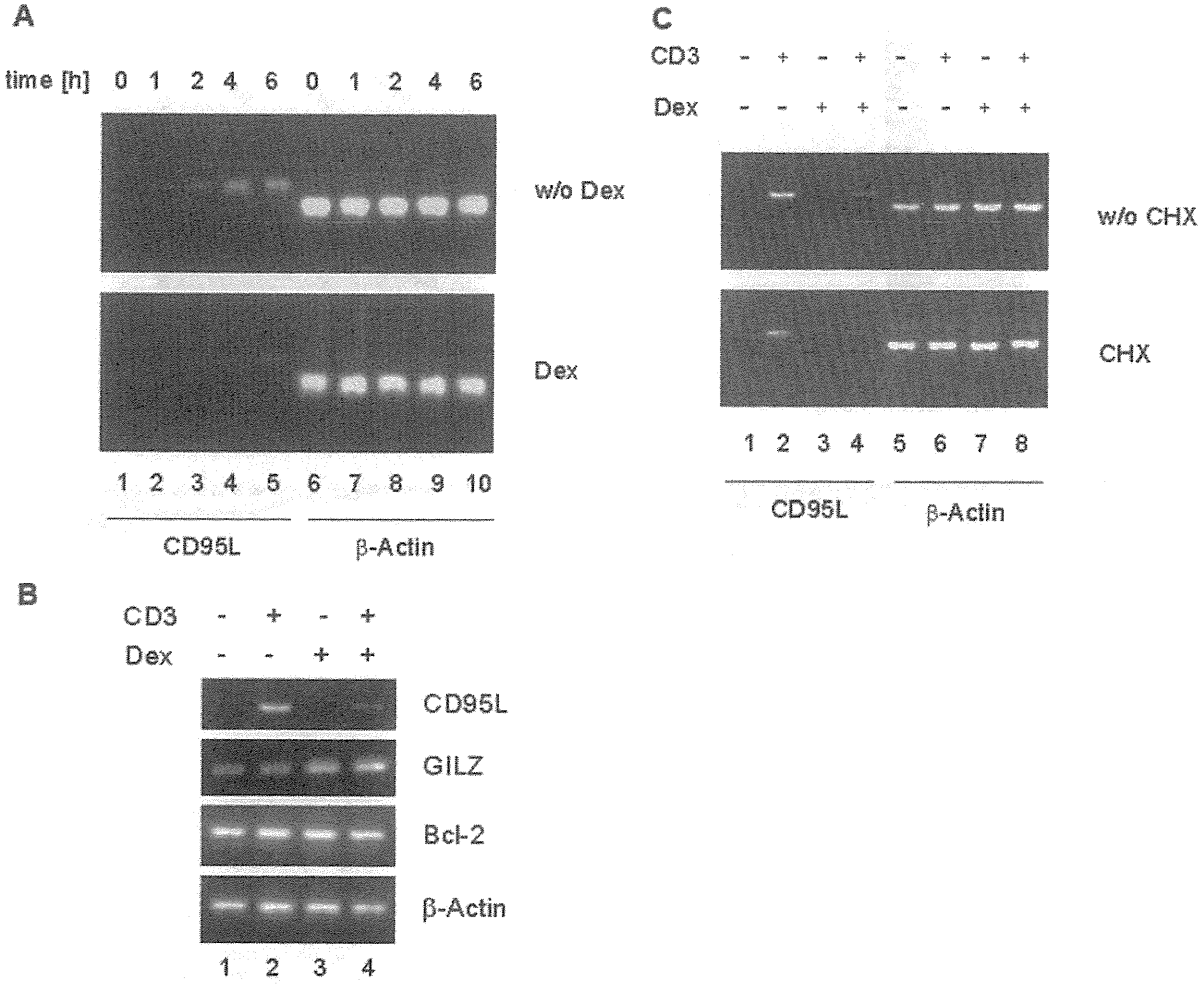

Figure 3. Dex-induced protein synthesis is not required for inhibition of CD95L mRNA expression. (A) Primary murine day-5 T cells were restimulated by anti-CD3 antibody in the presence or absence of 10^{-7} M Dex for the indicated periods of time. The mRNA expression level of CD95L and β-actin was detected by RT-PCR. (B) Primary murine day-5 T cells were restimulated by anti-CD3 antibody in the presence or absence of 10^{-7} M Dex for 5 hours. The mRNA expression of CD95L, GILZ, Bcl-2, and β-actin was detected by RT-PCR. (C) Same as in panel B, but restimulation with or without pretreatment for 2 hours with 10 μg/mL CHX. The mRNA expression of CD95L and β-actin was detected by RT-PCR. Results are representative of at least 3 independent experiments.

Kasama Y, Sekiguchi S, Saito M, et al. Persistent expression of the full genome of hepatitis C virus in B cells induces spontaneous development of B-cell lymphomas in vivo. *Blood.* 2010;116(23):4926-4933.

On page 4928 of the 2 December 2010 issue, the columns are misaligned in the graph in Figure 1B. The corrected Figure 1 is shown.

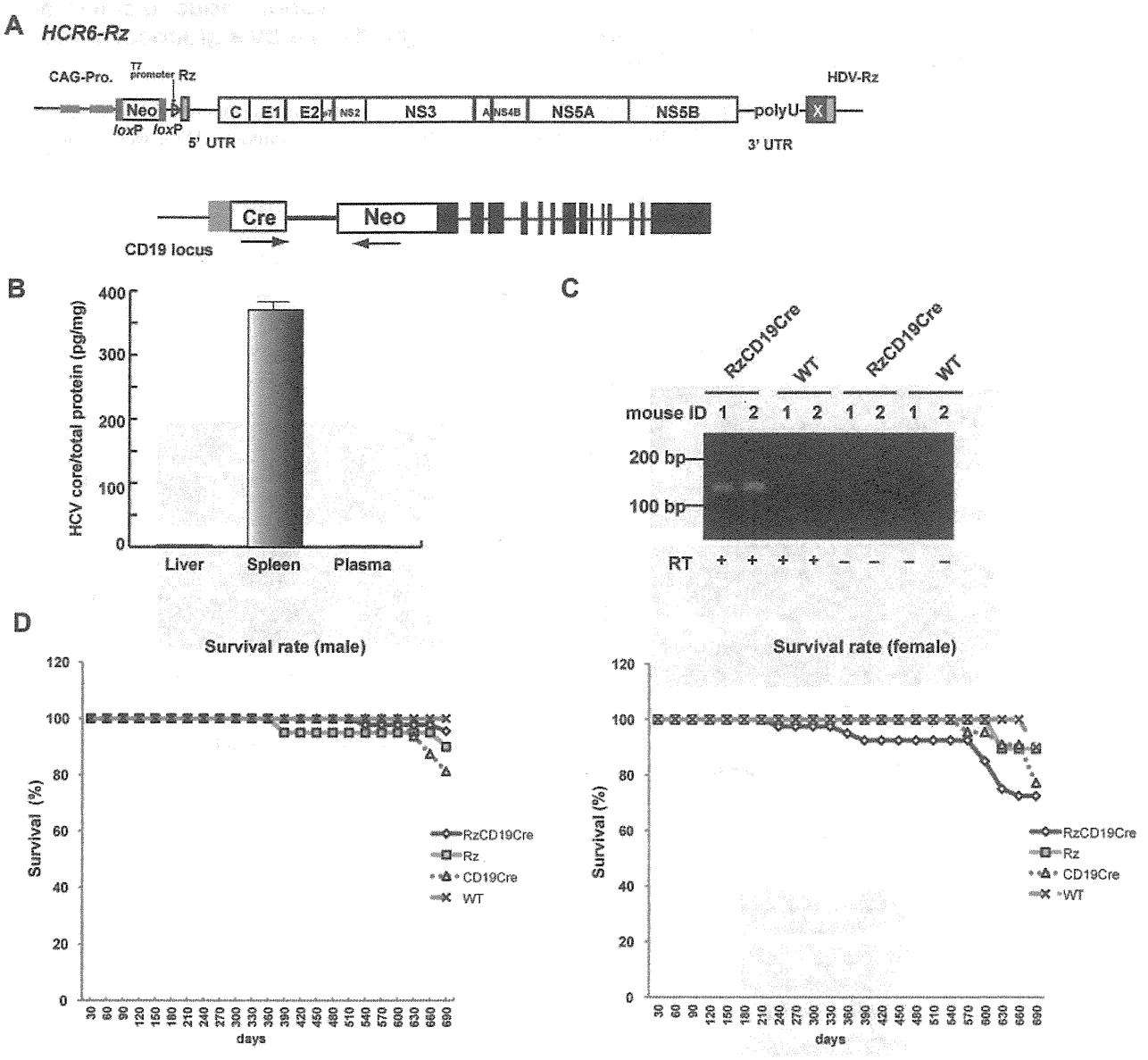

Figure 1. Establishment of RzCD19Cre mice. (A) Schematic diagram of the transgene structure comprising the complete HCV genome (*HCR6-Rz*). HCV genome expression was regulated by the Cre/*lox*P expression cassette (top diagram). The Cre transgene was located in the CD19 locus (bottom diagram). (B) Expression of HCV core protein in the liver, spleen, and plasma of RzCD19Cre mice was quantified by core ELISA. Data represent the mean ± SD (n = 3). (C) Detection of HCV RNA in PBLs by RT-PCR. Samples that included the RT reaction are indicated by +, and those that did not include the RT reaction are indicated by −. (D) Survival rates of male and female RzCD19Cre mice (males, n = 45; females, n = 40), Rz mice (males, n = 20; females, n = 19), CD19Cre mice (males, n = 16; females, n = 22), and WT mice (males, n = 5; females, n = 10).

Krauel K, Pötschke C, Weber C, et al. Platelet factor 4 binds to bacteria-inducing antibodies cross-reacting with the major antigen in heparin-induced thrombocytopenia. *Blood.* 2011;117(4):1370-1378.

On page 1370 in the 27 January 2011 issue, there is an error in punctuation in the title. The hyphenated word "bacteria-inducing" is incorrect. The title should have read: "Platelet factor 4 binds to bacteria, inducing antibodies cross-reacting with the major antigen in heparin-induced thrombocytopenia." The error was corrected in the online version, which now differs from the print version.

Leddin M, Perrod C, Hoogenkamp M, et al. Two distinct auto-regulatory loops operate at the PU.1 locus in B cells and myeloid cells. *Blood.* 2011;117(10):2827-2838.

On page 2827 in the 10 March 2011 issue, the superscript number indicating the affiliation for the eleventh author (Mosammam) is incorrect ([5]Department of Haematology, Cambridge Institute for Medical Research, University of Cambridge, Cambridge, United Kingdom). The correct superscript number is 2 and Mosammam's correct affiliation is [2]Leeds Institute for Molecular Medicine, University of Leeds, Leeds, United Kingdom. The error was corrected in the online version, which now differs from the print version.

JOURNAL OF VIROLOGY, Jan. 2010, p. 303–311
0022-538X/10/$12.00 doi:10.1128/JVI.01448-09

Vol. 84, No. 1

Pathogenesis of Hepatitis C Virus Infection in *Tupaia belangeri*▽†

Yutaka Amako,[1] Kyoko Tsukiyama-Kohara,[1,2] Asao Katsume,[1,3] Yuichi Hirata,[1] Satoshi Sekiguchi,[1] Yoshimi Tobita,[1] Yukiko Hayashi,[4] Tsunekazu Hishima,[4] Nobuaki Funata,[4] Hiromichi Yonekawa,[5] and Michinori Kohara[1]*

Department of Microbiology and Cell Biology, Tokyo Metropolitan Institute of Medical Science, 2-1-6, Kamikitazawa, Setagaya-ku, Tokyo 156-0057, Japan[1]; Department of Experimental Phylaxiology, Faculty of Medical and Pharmaceutical Sciences, Kumamoto University, 1-1-1 Honjo Kumamoto City, Kumamoto 860-8556, Japan[2]; Fuji Gotemba Research Laboratory, Chugai Pharmaceutical Company, Ltd., 135, Komakado 1 Chome, Gotemba-shi, Shizuoka 412-8513, Japan[3]; Department of Pathology, Tokyo Metropolitan Komagome Hospital, 3-18-22 Honkomagome, Bunkyo-ku, Tokyo 113-8677, Japan[4]; and Laboratory of Animal Science, Tokyo Metropolitan Institute of Medical Science, 2-1-6, Kamikitazawa, Setagaya-ku, Tokyo 156-0057, Japan[5]

Received 14 July 2009/Accepted 5 October 2009

The lack of a small-animal model has hampered the analysis of hepatitis C virus (HCV) pathogenesis. The tupaia (*Tupaia belangeri*), a tree shrew, has shown susceptibility to HCV infection and has been considered a possible candidate for a small experimental model of HCV infection. However, a longitudinal analysis of HCV-infected tupaias has yet to be described. Here, we provide an analysis of HCV pathogenesis during the course of infection in tupaias over a 3-year period. The animals were inoculated with hepatitis C patient serum HCR6 or viral particles reconstituted from full-length cDNA. In either case, inoculation caused mild hepatitis and intermittent viremia during the acute phase of infection. Histological analysis of infected livers revealed that HCV caused chronic hepatitis that worsened in a time-dependent manner. Liver steatosis, cirrhotic nodules, and accompanying tumorigenesis were also detected. To examine whether infectious virus particles were produced in tupaia livers, naive animals were inoculated with sera from HCV-infected tupaias, which had been confirmed positive for HCV RNA. As a result, the recipient animals also displayed mild hepatitis and intermittent viremia. Quasispecies were also observed in the NS5A region, signaling phylogenic lineage from the original inoculating sequence. Taken together, these data suggest that the tupaia is a practical animal model for experimental studies of HCV infection.

Hepatitis C virus (HCV) is a small enveloped virus that causes chronic hepatitis worldwide (32). HCV belongs to the genus *Hepacivirus* of the family *Flaviviridae*. Its genome comprises 9.6 kb of single-stranded RNA of positive polarity flanked by highly conserved untranslated regions at both the 5′ and 3′ ends (4, 27, 29). The 5′ untranslated region harbors an internal ribosomal entry site (29) that initiates translation of a single open reading frame encoding a large polyprotein comprising about 3,010 amino acids (35). The encoded polyprotein is co- and posttranslationally processed into 10 individual viral proteins (15).

In most cases of human infection, HCV is highly potent and establishes lifelong persistent infection, which progressively leads to chronic hepatitis, liver steatosis, cirrhosis, and hepatocellular carcinoma (9, 16, 21). The most effective therapy for treatment of HCV infection is administration of pegylated interferon combined with ribavirin. However, the combination therapy is an arduous regimen for patients; furthermore, HCV genotype 1b does not respond efficiently (19). The prevailing scientific opinion is that a more viable option than interferon treatment is needed.

The chimpanzee is the only validated animal model for in vivo studies of HCV infection, and it is capable of reproducing most aspects of human infection (5, 18, 23, 28, 35, 36). The chimpanzee is also the only validated animal for testing the authenticity and infectivity of cloned viral sequences (8, 14, 35, 36). However, chimpanzees are relatively rare and expensive experimental subjects. Cross-species transmission from infected chimpanzees to other nonhuman primates has been tested but has proven unsuccessful for all species evaluated (1).

The tupaia (*Tupaia belangeri*), a tree shrew, is a small nonprimate mammal indigenous to certain areas of Southeast Asia (6). It is susceptible to infection with a wide range of human-pathogenic viruses, including hepatitis B viruses (13, 20, 31), and appears to be permissive for HCV infection (33, 34). In an initial report, approximately one-third of inoculated animals exhibited acute, transient infection, although none developed the high-titer sustained viremia characteristic of infection in humans and chimpanzees (33). The short duration of follow-up precluded any observation of liver pathology. In addition to the putative in vivo model, cultured primary hepatocytes from tupaias can be infected with HCV, leading to de novo synthesis of HCV RNA (37). These reports strongly support tupaias as a valid model for experimental studies of HCV infection. However, longitudinal analyses evaluating the clinical development and pathology of HCV-infected tupaias have yet to be exam-

* Corresponding author. Mailing address: Department of Microbiology and Cell Biology, The Tokyo Metropolitan Institute of Medical Science, 2-1-6, Kamikitazawa, Setagaya-ku, Tokyo 156-0057, Japan. Phone: 81-3-5316-3232. Fax: 81-3-5316-3137. E-mail: kohara-mc@igakuken.or.jp.

† Supplemental material for this article may be found at http://jvi.asm.org/.

▽ Published ahead of print on 21 October 2009.

TABLE 1. Experimental HCV infections performed in this study

Tupaia no.	Inoculum		Biopsy/sacrifice[b]
	Type	Quantity (GE/tupaia)[a]	
Group I[c]			
Tup.4	RCV	1×10^7	84, 94/144 wk p.i.
Tup.5	HCR6	6×10^5	95, 105/155 wk p.i.
Tup.6	HCR6	6×10^5	95, 105/155 wk p.i.
Tup.8	RCV	1×10^7	84, 94/144 wk p.i.
Group II[d]			
Tup.9	Tup.5 (5 wk p.i.)	1×10^2	NT
Tup.10	Tup.5 (5 wk p.i.)	1×10^2	NT
Tup.11	Tup.8 (10 wk p.i.)	1×10^2	NT
Tup.12	Tup.8 (10 wk p.i.)	1×10^2	NT
Tup.13	Tup.4 (8 wk p.i.)	1×10^2	NT
Tup.14	Tup.4 (8 wk p.i.)	1×10^2	NT
Group III[e]			
Tup.15	None		92/100 wk
Tup.17	None		92/100 wk
Tup.38	None		242 wk
Tup.39	None		242 wk

[a] Viral RNA GE/tupaia was estimated by Quantitative real-time RT-PCR (GE, genome equivalents; sensitivity > 10 GE/ml serum).
[b] Liver biopsy was performed at indicated time-point. p.i., postinoculation; NT, not tested.
[c] Group I, primary infection experiment in which 1-year-old animals were inoculated with two different types of inocula.
[d] Group II, reinfection experiment, where HCV RNA-positive sera from Group I experimental infections were passaged to naive animals.
[e] GroupIII, no-infection control.

ined. In the present study, we describe the clinical development and pathology of HCV-infected tupaias over an approximately 3-year time course.

MATERIALS AND METHODS

Animals. Table 1 summarizes the tupaias used in this study. Tupaias born in laboratory captivity were obtained from the Laboratory Animal Center at the Kunming Institute of Zoology (Chinese Academy of Sciences). Tupaias were imported with permission from the Convention on International Trade in Endangered Species of Wild Fauna and Flora (7), quarantined for medical inspection, and housed individually in standard rat cages supplied with filtered air. The animals were fed a daily regimen of eggs, fruit, and the CMS-1 commercial diet for marmosets (CLEA, Japan). Their appetites and feces were carefully monitored. Animal care and experimental handling conformed to study guidelines established by the Subcommittee on Laboratory Animal Care at the Tokyo Metropolitan Institute of Science.

Patient serum used for animal infection. HCV genotype 1b serum, designated HCR6, was obtained from a patient with chronic active hepatitis C. The infectious titer of HCR6 was determined in chimpanzee and Molt4 cells and denoted plasma K (HCR6) by Shimizu et al. (24). The HCR6 serum exhibited a PCR titer of 6×10^6 genome equivalents/ml and an infectious titer of 3.7×10^4 50% chimpanzee infectious doses/ml. Serum aliquots were frozen at −80°C until they were used.

Virion reconstitution of cloned HCV. As described previously, pHCR6 (genotype 1b; 9,611 nucleotides; GenBank accession no. AY045720) is a plasmid carrying HCV genomic cDNA cloned from HCR6 serum (30). pHCR6Rz was designed for precisely trimmed RNA expression, with the entire genomic region of pHCR6Rz recloned under the control of the T7 promoter and the 5′ and 3′ distal ends flanked by hammerhead- and hepatitis D virus ribozyme-encoding sequences, respectively (22, 25).

For molecular reconstitution of HCV particles, pHCR6Rz was transfected into IMY-N9 cells as described previously (12). Briefly, semiconfluent IMY-N9 cells in 100-mm plastic dishes were transfected with 15 μg of plasmid using 40 μl of cationic lipids (DMRIE-C reagent; Life Technology) in accordance with the manufacturer's instructions. Five hours after transfection, the cells were infected with AdexCAT7 (2) (kindly provided by Y. Matsuura) at a multiplicity of infection of 20. After infection, the culture medium was replaced with Hepato-STIM (Becton Dickinson). The culture supernatants were collected at 24 h postinfection and stored at −80°C.

Virus inoculation and collection of serum samples. Animals were infected at 6 months of age. The anesthetic agent, ketamine hydrochloride, was administered intramuscularly at 50 mg/kg body weight prior to virus inoculation and bleeding of the tupaias. The inocula were introduced intravenously at 6×10^5 genome equivalents/animal for patient serum HCR6 and 1×10^7 genome equivalents/animal for reconstituted virions derived from the pHCR6Rz inoculation. Blood samples were drawn from infected and control animals pre- and postinfection. Briefly, the animals were bled weekly for 20 weeks and biweekly thereafter. At each time point, 0.5 ml of blood was drawn from the thigh vein; the sera were separated, aliquoted, and stored for subsequent assays.

Reinfection experiments were performed by transmission of HCV RNA-positive serum from group I (Table 1) to naive animals.

Serum alanine aminotransferase (ALT) concentrations were determined using a Transnase Nissui kit (Nissui Pharmaceutical Co.), standardized, and displayed as IU/liter.

RNA isolation and quantitative RTD-PCR assay for HCV RNA. Serum samples (100 μl) were tested for circulating HCV RNA in vivo using quantitative real-time detection (RTD)-PCR (TaqMan). RNA was extracted from the sera and livers of sacrificed animals using the acid guanidium-phenol chloroform method with tRNA as a carrier (3). Two tupaias (Tup.5 and Tup.6) were inoculated with patient serum HCR6. Another two animals (Tup.4 and Tup.8) were inoculated with reconstituted viral particles (RCV). Tup.15 served as a mock-infected control. Liver specimens (3- to 4-mm^2 blocks) from these tupaias were homogenized with 1.5 ml of 5 M guanidine thiocyanate using a polytron-type homogenizer (Ultra-Turrax T25; IKA Laborteehnik, Staufen, Germany). RNA was then reextracted with 4 M guanidine thiocyanate.

RNA samples were subjected to RTD-PCR on an ABI 7700 sequence detector (Applied Biosystems) as described previously (26). The extracted RNA was dissolved in 200 μl of diethyl pyrocarbonate-treated water containing 10 mM dithiothreitol and 200 units/ml RNase inhibitor in a siliconized tube. RTD-PCR was performed using 1 μg of total RNA, one set of PCR primers, and a probe for a location within the 5′ noncoding region using the EZ r*Tth* RNA PCR kit (Perkin Elmer) and the ABI Prism 7700 sequence detector system. A standard curve was constructed using a 10-fold dilution series of in vitro-transcribed and previously titrated synthetic HCV RNA.

Consequently, the quantities represented by genome equivalents correspond to an absolute standard curve (26). All quantitative RTD-PCR assays were performed using duplicate samples, with both negative control serum and HCV-positive serum included. The control sera were diluted before use and were estimated to contain low copy numbers of HCV RNA (100 genome equivalents/ml serum). Samples were deemed positive for HCV RNA if both duplicates yielded PCR-amplified product. Averages of the two estimated values are shown in the figures.

Histological analysis. Tissue samples were carefully collected from anesthetized animals by abdominal incision, fixed in 10% neutral buffered formalin, embedded in paraffin, sectioned, and stained with hematoxylin and eosin (H&E). Silver and Sudan IV (Wako Pure Chemical Industries, Ltd.) staining were also carried out to visualize fiber generation and lipid degeneration, respectively. All histological staining was performed in accordance with conventional procedures. The histological status was determined using the modified hepatitis activity index scoring system, which grades necrosis and inflammation on a scale of 0 to 18 (periportal inflammation and necrosis, 0 to 10; lobular inflammation and necrosis, 0 to 4; portal inflammation, 0 to 4) (11). Fibrosis was scored using the Ishak fibrosis scale of 0 to 6 (0, no fibrosis; 1 or 2, portal fibrosis; 3 or 4, bridging fibrosis; and 5 or 6, cirrhosis). The values in each group (Table 2) represent the averages of the scores in five visual fields.

Statistical analysis. The statistical significance of differences between controls and HCV-infected animals was analyzed with the nonparametric Mann-Whitney U test. All comparisons were two tailed. The statistical analysis was conducted with SPSS 12.0 software (SPSS Inc., Chicago, IL).

RESULTS

Inoculation of HCV causes acute hepatitis and transient viremia in tupaias. To begin this study, two distinct but related inocula were chosen for infection of tupaias. Serum from a chronic hepatitis patient (designated HCR6) was chosen for its

TABLE 2. Grading: necroinflammatory scores and fibrosis

Group	Inoculum	Tupaia no.	Grade				Total	Avg	SD	Staging
			A	B	C	D				
94 wk p.i. (biopsy)										
I	HCR 6	Tup.5	0	0	0	0	0	1.3	1.5	0
		Tup.6	1	0	1	0	2			0
	RCV	Tup.4	0	0	0	0	0			0
		Tup.8	0	0	0	3	3			6
	Control	Tup.15	0	0	0	0	0	0	0	0
III		Tup.17	0	0	0	0	0			0
		Tup.38								
		Tup.39								
144 wk p.i. (sacrifice)										
I	HCR 6	Tup.5	1	0	2	3	6	5.5	3.7	0
		Tup.6	3	0	4	3	10			1
	RCV	Tup.4	0	0	0	1	1			0
		Tup.8	1	0	1	3	5			6
	Control	Tup.15						0	0	
III		Tup.17								
		Tup.38	0	0	0	0	0			0
		Tup.39	0	0	0	0	0			0

defined genotype (genotype 1b), and genetic heterogeneity was ascertained by the process of cloning consensus cDNA. The infectivity of this serum was also experimentally defined in chimpanzees; a 50% chimpanzee infectious dose was estimated at 3.7×10^4 50% chimpanzee infectious doses/ml. Furthermore, the consensus genomic sequence of HCV was cloned from the serum (pHCR6; 9,611 bases; GenBank AY045702.1). For the second inoculum (referred to as RCV), clonal viral particles were reconstituted as described in Materials and Methods. This inoculum was expected to be free of neutralizing antibodies and thus was considered potentially more infectious than patient sera. In the case of RCV infection, genetic diversification of viral RNA, also known as quasispecies, can be regarded as a direct indication of de novo synthesis of progenitor virus in vivo.

Either patient serum or cDNA-derived RCV was inoculated into tupaias (Table 1, group I). Two animals (one female and one male) were tested against each inoculum. Age-matched animals were bred as infection-free controls.

All experimental infections are described in Materials and Methods and Table 1. Prior to experimental infection, the normal serum ALT level in tupaias was measured at 22.3 IU/liter ($n = 23$).

Inoculation with patient serum HCR6 caused rapid fluctuations in the serum ALT concentrations, from two- to fivefold, in both inoculated tupaias, suggesting acute hepatitis in vivo (Fig. 1A and B). Correlative quantitative RTD-PCR revealed HCV viremia soon after serum inoculation in Tup.5, which continued to show transient viremia long term. The appearance of viremia sometimes coincided with a steep elevation in the serum ALT (Fig. 1A). Conversely, HCV RNA was not detected in the serum of Tup.6 up to 60 weeks postinoculation and only twice thereafter. Acute-phase ALT elevations (3 to 4 weeks postinoculation) in Tup.6 might represent tight control of HCV infection by the host immune system (Fig. 1B).

Distinct results were obtained for the two animals (Tup.4 and Tup.8) inoculated with RCV. Both animals displayed sustained viremia up to 10 weeks postinoculation (Fig. 1C and D), indicating persistent HCV infection and inability to eradicate the virus. Viremia was detected intermittently throughout the course of infection, sometimes accompanying the elevation of serum ALT. Humoral immune responses in Tup.5 and Tup.6 (see Fig. S1A in the supplemental material) and Tup.4 and Tup.6 (see Fig. S1B in the supplemental material) were indicated.

We performed RTD-PCR to confirm whether HCV could replicate in the tupaias' livers (Tup.4, Tup.5, Tup.6, and Tup.8) and obtained the following results (Fig. 1E): 310 ± 117 copies/μg total RNA in Tup.5, 80 ± 11 copies/μg in Tup.6, 199 ± 77 copies/μg in Tup.4, and 292 ± 48 copies/μg in Tup.8. In contrast, HCV RNA was not detected in the liver of the mock-infected animal (Tup.15).

HCV RNA was also not detected in samples from either preinoculation or age-matched, infection-free control tupaias (Table 1, group III), nor were significant elevations in serum ALT observed for any of the three infection-free controls (data not shown).

HCV causes chronic hepatitis in tupaia liver, leading to fibrosis and cirrhosis. Serum ALT and circulating HCV RNA levels in primary infected tupaias (Table 1, group I) were monitored for 3 years postinoculation. As described above, the magnitudes of serum ALT fluctuations varied substantially among infected animals (Fig. 1A, B, C, and D). Tupaia livers were examined for histological lesions in order to elucidate if HCV caused chronic hepatitis. Liver biopsies via abdominal incisions were performed at 2 years postinoculation. All animals were sacrificed at 3 years postinoculation (4.5 years for uninfected animals). H&E staining of liver specimens from HCV-infected tupaias showed infiltrating lymphocytes within sinusoids and around portal areas, indicating chronic hepatitis in the tupaia livers (Fig. 2B, D, and H). Infiltrating lymphocytes were also observed in limiting plates, indicating ongoing inflammation (Fig. 2G and H). Furthermore, a comparison of liver samples at 2 and 3 years postinoculation revealed that the

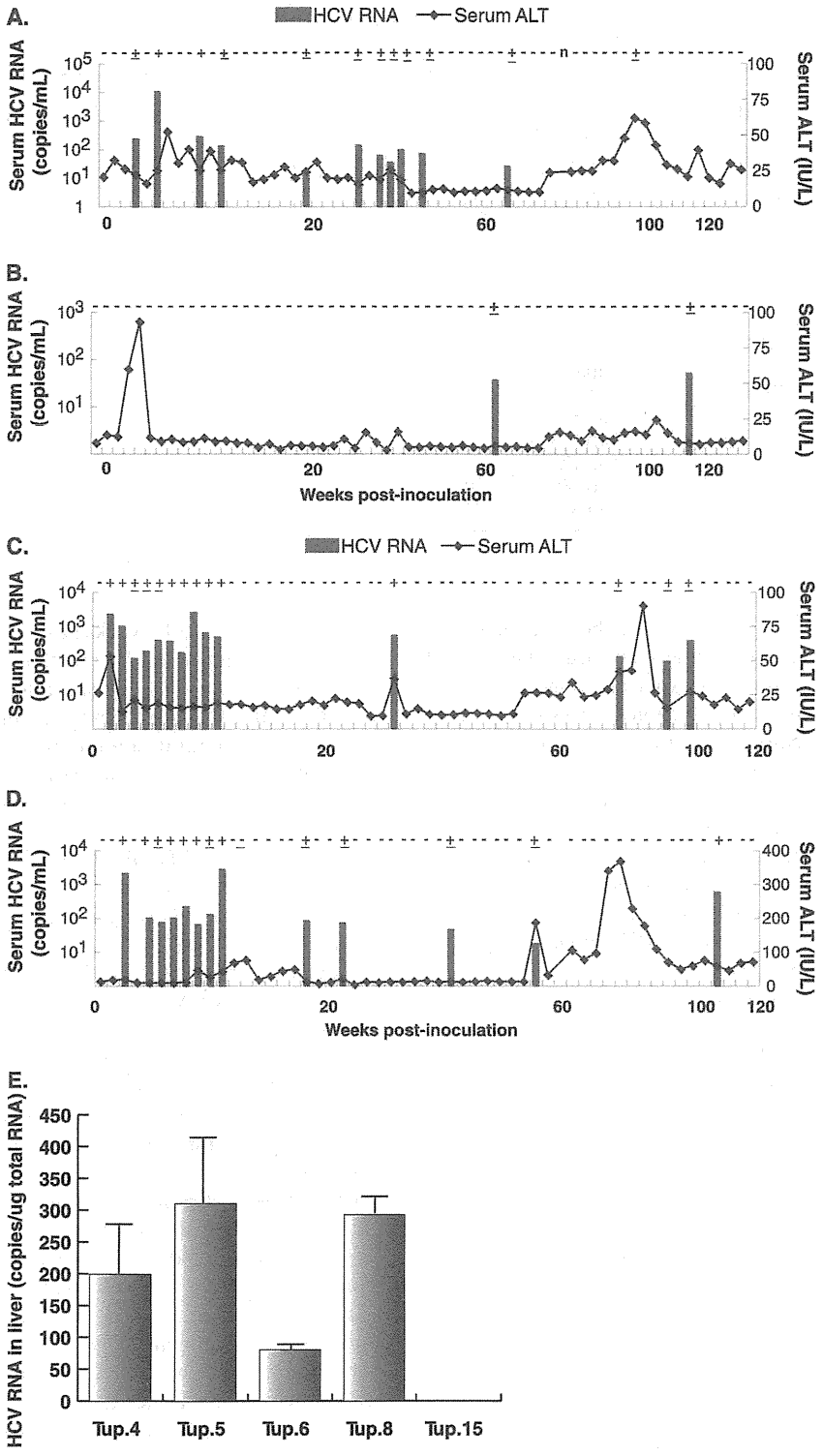

FIG. 1. Course of infection with patient serum HCR6 and RCV. (A) The results of quantitative RTD-PCR for HCV RNA and serum ALT concentrations were combined and plotted to show the course of infection in Tup.5. The bars and the ordinates on the left represent HCV RNA as genome equivalents/ml of serum. The curved line and the ordinates on the right represent serum ALT concentrations as IU/liter serum. (B) Serum HCV RNA and ALT concentrations for infection of Tup.6. (C) The graph for Tup.4. (D) The graph for Tup.8. The vertical axis for serum ALT in this graph is scaled differently from the others because of significant ALT elevation. (E) Quantification of HCV RNA in tupaia liver. HCV RNA in hepatocytes from tupaia (Tup.4, Tup.5, Tup.6, Tup.8, and Tup.15) livers was isolated 172 weeks after HCV infection and quantified by RTD-PCR. As few as 10 copies of the genome were detected, and the quantification range was between 10^1 and 10^8 copies (26).

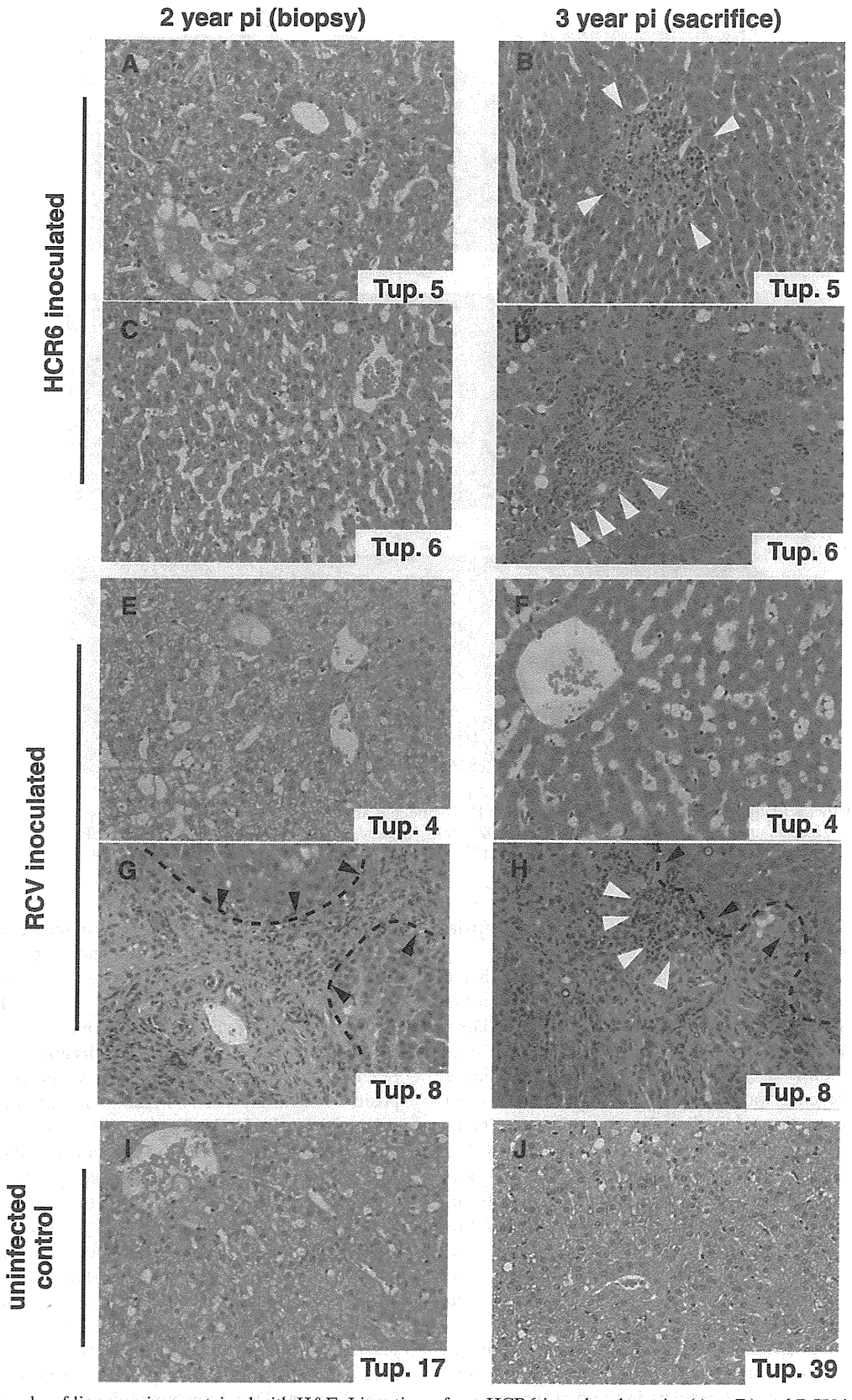

FIG. 2. Micrographs of liver specimens stained with H&E. Liver tissue from HCR6-inoculated tupaias (A to D) and RCV-inoculated tupaias (E to H) was obtained at 2 and 3 years postinoculation (pi). (I and J) Liver specimens from uninfected animals age matched to each inoculated animal were also obtained. The HCV-infected tupaia livers harbored infiltrating lymphocytes (white arrowheads) and fibrosis (broken lines and black arrowheads), which indicate chronic hepatitis.

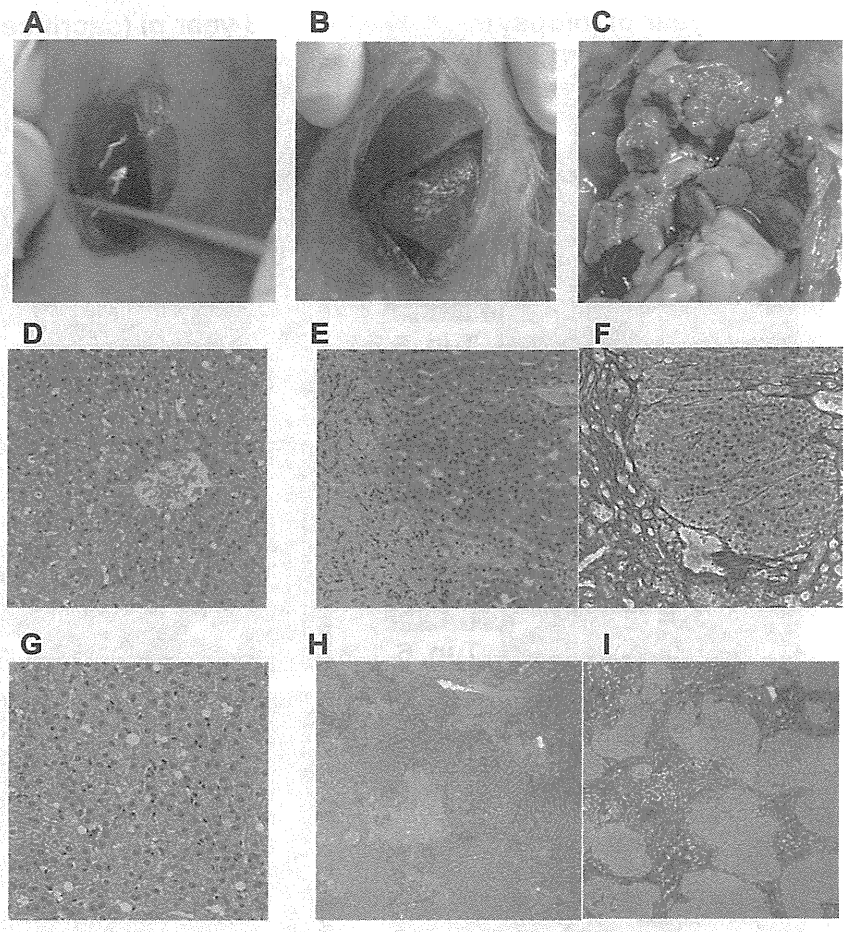

FIG. 3. Macro- and microscopic features of tupaia liver. (A) Infection-free control tupaia (Tup.15; 92 weeks). (B) RCV-infected animal displaying liver cirrhosis (Tup.8; 84 weeks postinoculation). (C) RCV-infected animal with massive surface nodules (Tup.8; 144 weeks postinoculation). (D and G) H&E staining of the uninfected Tup.15 at 92 weeks (D) and the uninfected Tup.39 at 242 weeks (G). (E, F, H, and I) H&E and silver staining of Tup.8 at 84 weeks postinoculation (E and F) or at 144 weeks postinoculation (H and I).

hepatitis had worsened with time in all HCV-infected tupaias (Fig. 2A to H and Table 2).

Fibrosis and cirrhosis were also examined. Mild fibrosis was seen in Tup.6, while severe fibrosis was seen in Tup.8. Cirrhosis was histologically investigated in all animals (Table 2). There was no significant difference between groups I and III at 94 weeks postinfection ($P = 0.194$), but at 144 weeks postinfection, a slight difference was observed ($P = 0.059$; SPSS 12.0). Macroscopic observation of the liver biopsy specimens (taken 2 years postinoculation) indicated liver cirrhosis in Tup.8 (Fig. 3B) compared with Tup.15 (uninfected control) (Fig. 3A), while silver staining of histology samples revealed fibrosis and cirrhotic nodules (Fig. 3E and F). Macroscopic observation upon sacrifice (3 years postinoculation) indicated that liver cirrhosis in Tup.8 had worsened (Fig. 3C). In contrast, age-matched infection-free negative control tupaias displayed none of these pathologies (Fig. 3A, D, and G).

Progressive lipid degeneration was noted in infected tupaias throughout the course of infection (Fig. 4). In particular, Tup.5 displayed microvesicular lipid droplets in the first biopsy specimens (at 2 years), which developed into macrovesicular droplets and foamy degeneration in biopsy specimens at 3 years (Fig. 4C and D). Liver specimens from other infected animals displayed intracellular micro- and macrovesicular lipid droplets in hepatocytes at 3 years postinoculation (Fig. 4F, H, and J). These anomalies were not present in liver specimens from infection-free control animals (Fig. 4A and B).

Transmission of viral-RNA-positive serum to naive animals reproduces acute hepatitis and viremia. To confirm virion regeneration in vivo, and to exclude the possibility of false-positive serum HCV RNA results due to amplification of the original inocula, HCV RNA-positive sera from primary inoculated tupaias were used to inoculate naive tupaias. Three different sera were tested in this passage experiment, with two naive tupaias used as recipient animals for each trial (see Materials and Methods) (Table 1, group II).

In the first reinfection experiment, serum from Tup.5 (originally infected with patient serum HCR6) was collected at 5 weeks postinoculation and used to infect two naive animals. The recipient animals showed intermittent viremia over the subsequent 3 months (Fig. 5A). In the second and third cases of reinfection, sera from Tup.8 at 10 weeks postinoculation and from Tup.4 at 8 weeks postinoculation also induced viremia in the naive inoculated animals, similar to the first reinfection experiment (Fig. 5B and C). Furthermore, the PCR titers of the recipient tupaias were significantly greater than the inoc-

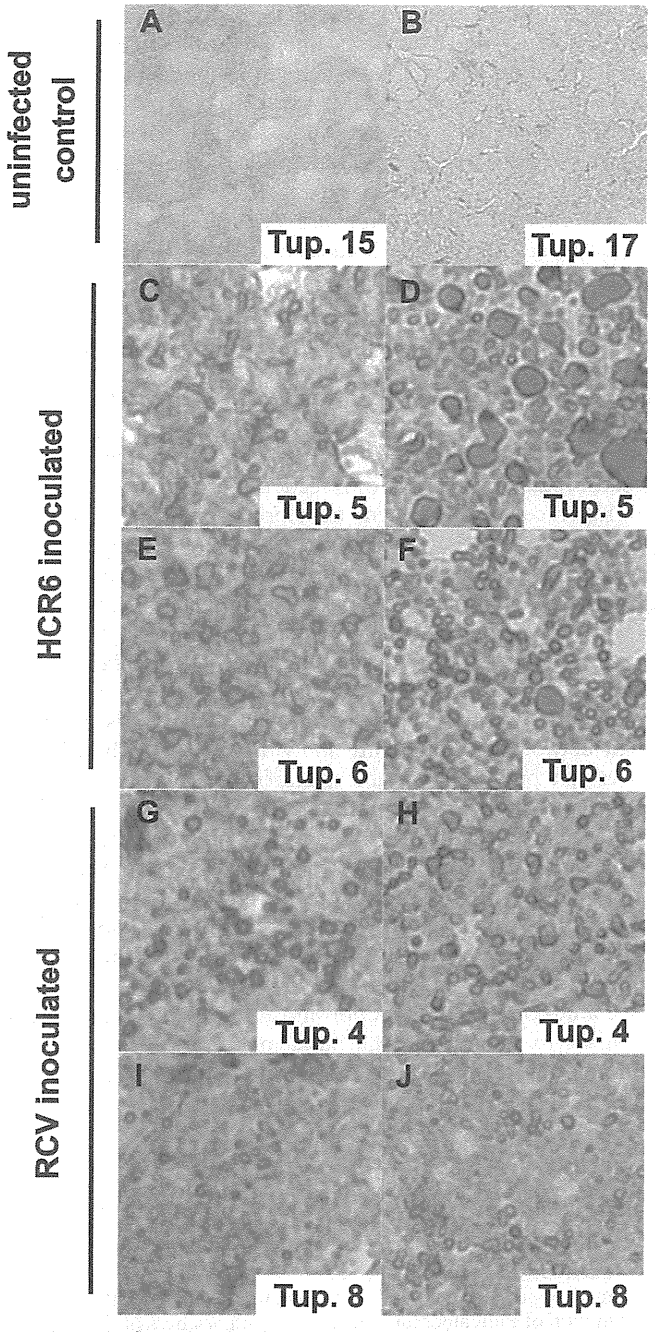

FIG. 4. Sudan IV-stained liver specimens exhibiting fatty liver degeneration. Cryosections of liver stained by Sudan IV as described in Materials and Methods show fatty liver degeneration. The left and right columns display biopsy specimens of infected animals (2 years postinoculation) and animals sacrificed at 3 years postinfection, respectively. (A and B) Uninfected controls at 2 years (Table 1 shows sample timing). (C to F) Patient serum HCR6-infected animals. (G to J) RCV-infected animals.

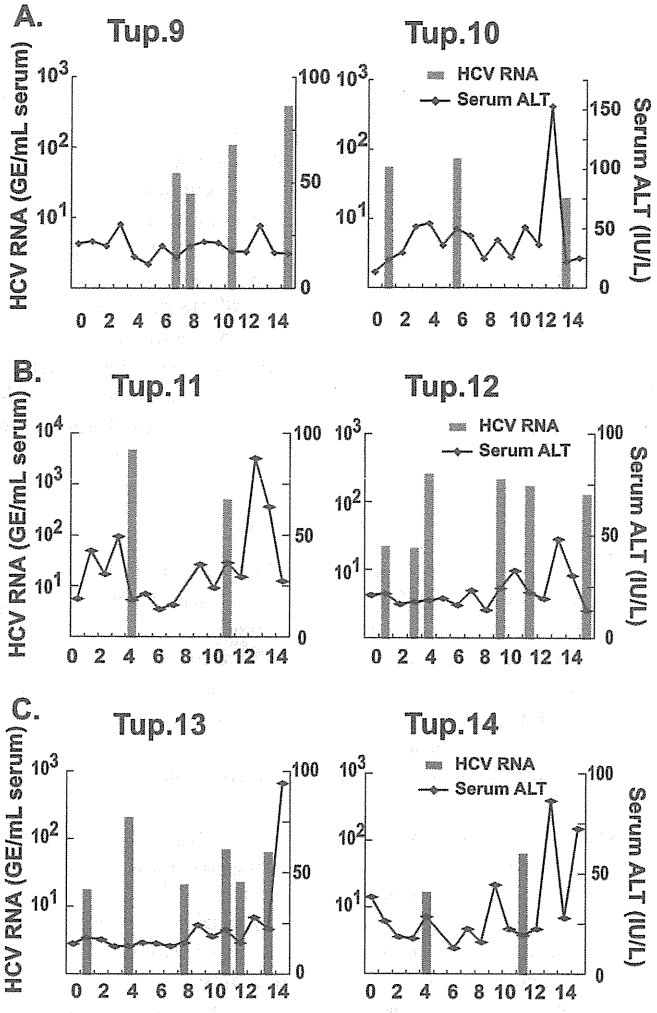

FIG. 5. Results of a reinfection experiment. (A) Quantitative RTD-PCR for HCV RNA and serum ALT levels are shown. Two naive animals were inoculated with tupaia serum (using serum taken at 5 weeks postinoculation from Tup.5, originally inoculated with patient serum HCR6) containing 100 genome equivalents (GE)/ml and were monitored for 15 weeks postinoculation (Table 1). (B) Tupaia serum (taken at 10 weeks postinoculation from Tup.8, originally inoculated with RCV) that was positive for HCV RNA was passaged into two naive animals. The animals were inoculated with tupaia serum at 100 GE/animal and monitored for 15 weeks postinoculation. (C) Tupaia serum (taken at 8 weeks postinoculation from Tup.4, originally inoculated with RCV) that was positive for HCV RNA was passaged into naive animals. The animals were inoculated with serum at 100 GE/animal and monitored for 20 weeks postinoculation.

ulation titers (10^2 genome equivalents/animal) (Table 1). For Tup.11, serum from 4 weeks postinoculation contained almost 10^4 genome equivalents/ml of HCV RNA (Fig. 5B). In addition, significant increases in serum ALT accompanied detection of serum HCV RNA. These results indicate that HCV RNA-positive sera from group I actually contained infectious virion particles. They also suggest that reconstituted HCV particles made from cDNA are infectious in tupaias.

We amplified a portion of the NS5A sequence, which is known as the interferon sensitivity determining region, by reverse transcription-PCR as described in the supplemental material. Each PCR product was subcloned and sequenced to compare the encoded amino acid sequences. For the purposes of this study, animals were inoculated with a molecular clonal virus consisting of a unique viral sequence of cDNA. The interferon sensitivity determining region sequences recovered from an animal infected with clonal inoculum (Tup.8 at 103 weeks postinoculation) were found to be heterogeneous, with

a few amino acid substitutions (K2212M for 2/10 cases, L2232P for 1/10 cases, and L2253S for 6/10 cases) (see Fig. S2E in the supplemental material). Interestingly, the codon for amino acid 2224 encodes valine, but it was found to be variant for alanine and valine in sequences from the original patient serum (HCR6). Tupaias infected with patient serum also exhibited variability at position 2224; valine occupancy was rare, as was seen in the original HCR6 population (see Fig. S2B and C in the supplemental material). On the other hand, this position was occupied solely by valine for sequences recovered from Tup.8 (see Fig. S2E in the supplemental material), indicating that genetic variations shown for Tup.8 originated from the pHCR6 cDNA sequence. Taken together, quasispecies detection of circulating virus represents further evidence demonstrating intrinsic replication of HCV in tupaias despite low levels and infrequent detection of viremia.

DISCUSSION

In the present study, we described persistent HCV infection in tupaias. Long-term follow-up was performed and revealed histological progression of HCV-related liver disorders in infected tupaias, including steatosis, fibrosis, and cirrhosis, in addition to acute and chronic hepatitis. HCV genomic RNA was detected in animal sera intermittently throughout the entire course of infection. However, HCV RNA was detected in the liver upon sacrifice (3 years postinoculation). Furthermore, HCV RNA in serum contained genomic variants that had diverged from the inoculated virus (see Fig. S1 and S2 in the supplemental material). These data strongly indicate an established persistent infection in the tupaias studied. All animals exhibited HCV viremia soon after inoculation, yet the viremia was intermittent and accompanied by relatively low RTD-PCR titers compared with equivalent human and chimpanzee infections. The discrepancy between humans and tupaias might be due to host-dependent differences in replication efficiency. Over the course of HCV infection in these tupaias, serum ALT profiles indicated repeated liver injury, probably due to host immune responses mediated by agents such as cytotoxic T lymphocytes rather than direct viral cytopathic effects.

In cases of tupaia infection, experimental inoculations rarely led to sustained viremia, which for most human cases lasts for the entire course of infection. Even the course of infection appeared transient and self-resolved. It seems likely that HCV replication is less compatible with the tupaia host environment. This possibility was substantiated by a previous report by Xu et al. (34), where tissue-cultured virions of cloned genotype 1b, referred to as HCVcc in the paper, could not cause chronic infection with sustained viremia in tupaias. Although HCVcc actually infected most of the inoculated tupaias (83%; 10/12), chronic infection was seen for only a fraction of them (20%; 2/10). In this study, we also tried to detect a humoral response to HCV core antigen. We found that tupaia sera were HCV positive for antibodies only at occasional time points, observable as intermittent steep responses (data not shown). Overall, sustained seroconversion was not seen in this study, probably because HCV propagation in vivo was so limited or well controlled by host immunity. Given that models of HCV propagation are severely limited, the most important and interesting finding of this study is the successful detection of HCV RNA in livers of infected tupaias 3 years after inoculation, indicating that HCV persists in tupaias. Although the limited propagation of HCV in tupaias is a drawback of this model at the present time, the isolation of tupaia-adapted HCV may be feasible by performing multiple infection passages. This possibility is supported by both quasispecies development and successful reinfection.

The chimpanzee is the animal species most closely related to humans, and as a model, it has contributed significantly to our understanding of HCV infection and pathogenesis. However, reproducing HCV pathogenesis in humans or chimpanzees can take as long as 10 to 20 years. The chronically infected tupaias in the present study developed complicated liver disorders in a much shorter time. Using tupaias, with their relatively short life span (3 to 5 years in the laboratory), as a model of HCV infection, we can evaluate HCV pathogenesis and correlate senescence and duration of infection.

The recent development of a primary human hepatocyte xenograft-uPA/SCID mouse model opened up opportunities to test putative antivirals against HCV replication in vivo (10, 17). In this innovative model, human hepatocytes, which are transplanted into the lobe of a mouse liver, can support HCV replication effectively. As a result, the level of circulating HCV RNA is comparable to that of a human patient. However, this mouse model is immunodeficient, and thus, it lacks the interplay between host immunity and viral infection. Therefore, it does not provide a suitable platform for characterizing immune responses to HCV infection.

HCV infection in tupaias represents an important model of HCV infection, particularly for the study of key determinants controlling virus propagation in vivo. The pathogenesis of HCV infection can be substantially different among humans, chimpanzees, and tupaias, and the mechanisms governing these differences are of great interest. Comparative studies of HCV infection in these different species will help us to understand the basic mechanisms of persistent infection.

ACKNOWLEDGMENTS

We thank Masahiro Shuda for helpful assistance and Etsuko Endo for creating the figures. We also thank the staffs of the Departments of Microbiology and Cell Biology and Mitsugu Takahashi for breeding the tupaias.

This study was supported by grants from the Ministry of Education, Culture, Sports, Science and Technology of Japan; the Program for Promotion of Fundamental Studies in Health Sciences of the Pharmaceuticals and Medical Devices Agency of Japan; and the Ministry of Health, Labor and Welfare of Japan.

REFERENCES

1. **Abe, K., T. Kurata, Y. Teramoto, J. Shiga, and T. Shikata.** 1993. Lack of susceptibility of various primates and woodchucks to hepatitis C virus. J. Med. Primatol. **22:**433–434.
2. **Aoki, Y., H. Aizaki, T. Shimoike, H. Tani, K. Ishii, I. Saito, Y. Matsuura, and T. Miyamura.** 1998. A human liver cell line exhibits efficient translation of HCV RNAs produced by a recombinant adenovirus expressing T7 RNA polymerase. Virology **250:**140–150.
3. **Chomczynski, P., and N. Sacchi.** 1987. Single-step method of RNA isolation by acid guanidinium thiocyanate-phenol-chloroform extraction. Anal. Biochem. **162:**156–159.
4. **Choo, Q. L., G. Kuo, A. J. Weiner, L. R. Overby, D. W. Bradley, and M. Houghton.** 1989. Isolation of a cDNA clone derived from a blood-borne non-A, non-B viral hepatitis genome. Science **244:**359–362.
5. **Dash, S., G. Kalkeri, H. M. McClure, R. F. Garry, S. Clejan, S. N. Thung, and K. K. Murthy.** 2001. Transmission of HCV to a chimpanzee using virus

particles produced in an RNA-transfected HepG2 cell culture. J. Med. Virol. **65:**276–281.
6. **Flugge, P., E. Fuchs, E. Gunther, and L. Walter.** 2002. MHC class I genes of the tree shrew Tupaia belangeri. Immunogenetics **53:**984–988.
7. **Goldsmith, E. I.** 1978. The convention on international trade in endangered species of wild fauna and flora. J. Med. Primatol. **7:**122–124.
8. **Hong, Z., M. Beaudet-Miller, R. E. Lanford, B. Guerra, J. Wright-Minogue, A. Skelton, B. M. Baroudy, G. R. Reyes, and J. Y. Lau.** 1999. Generation of transmissible hepatitis C virions from a molecular clone in chimpanzees. Virology **256:**36–44.
9. **Hoofnagle, J. H.** 2002. Course and outcome of hepatitis C. Hepatology **36:**S21–S29.
10. **Inoue, K., T. Umehara, U. T. Ruegg, F. Yasui, T. Watanabe, H. Yasuda, J. M. Dumont, P. Scalfaro, M. Yoshiba, and M. Kohara.** 2007. Evaluation of a cyclophilin inhibitor in hepatitis C virus-infected chimeric mice in vivo. Hepatology **45:**921–928.
11. **Ishak, K., A. Baptista, L. Bianchi, F. Callea, J. De Groote, F. Gudat, H. Denk, V. Desmet, G. Korb, R. N. MacSween, et al.** 1995. Histological grading and staging of chronic hepatitis. J. Hepatol. **22:**696–699.
12. **Ito, T., K. Yasui, J. Mukaigawa, A. Katsume, M. Kohara, and K. Mitamura.** 2001. Acquisition of susceptibility to hepatitis C virus replication in HepG2 cells by fusion with primary human hepatocytes: establishment of a quantitative assay for hepatitis C virus infectivity in a cell culture system. Hepatology **34:**566–572.
13. **Kock, J., M. Nassal, S. MacNelly, T. F. Baumert, H. E. Blum, and F. von Weizsacker.** 2001. Efficient infection of primary tupaia hepatocytes with purified human and woolly monkey hepatitis B virus. J. Virol. **75:**5084–5089.
14. **Kolykhalov, A. A., E. V. Agapov, K. J. Blight, K. Mihalik, S. M. Feinstone, and C. M. Rice.** 1997. Transmission of hepatitis C by intrahepatic inoculation with transcribed RNA. Science **277:**570–574.
15. **Major, M. E., and S. M. Feinstone.** 1997. The molecular virology of hepatitis C. Hepatology **25:**1527–1538.
16. **Marcellin, P., T. Asselah, and N. Boyer.** 2002. Fibrosis and disease progression in hepatitis C. Hepatology **36:**S47–S56.
17. **Mercer, D. F., D. E. Schiller, J. F. Elliott, D. N. Douglas, C. Hao, A. Rinfret, W. R. Addison, K. P. Fischer, T. A. Churchill, J. R. Lakey, D. L. Tyrrell, and N. M. Kneteman.** 2001. Hepatitis C virus replication in mice with chimeric human livers. Nat. Med. **7:**927–933.
18. **Nascimbeni, M., E. Mizukoshi, M. Bosmann, M. E. Major, K. Mihalik, C. M. Rice, S. M. Feinstone, and B. Rehermann.** 2003. Kinetics of CD4+ and CD8+ memory T-cell responses during hepatitis C virus rechallenge of previously recovered chimpanzees. J. Virol. **77:**4781–4793.
19. **Pawlotsky, J. M.** 2002. Use and interpretation of virological tests for hepatitis C. Hepatology **36:**S65–S73.
20. **Ren, S., and M. Nassal.** 2001. Hepatitis B virus (HBV) virion and covalently closed circular DNA formation in primary tupaia hepatocytes and human hepatoma cell lines upon HBV genome transduction with replication-defective adenovirus vectors. J. Virol. **75:**1104–1116.
21. **Seeff, L. B.** 2002. Natural history of chronic hepatitis C. Hepatology **36:**S35–S46.
22. **Shimayama, T., S. Nishikawa, and K. Taira.** 1995. Generality of the NUX rule: kinetic analysis of the results of systematic mutations in the trinucleotide at the cleavage site of hammerhead ribozymes. Biochemistry **34:**3649–3654.
23. **Shimizu, Y. K., H. Igarashi, T. Kanematu, K. Fujiwara, D. C. Wong, R. H. Purcell, and H. Yoshikura.** 1997. Sequence analysis of the hepatitis C virus genome recovered from serum, liver, and peripheral blood mononuclear cells of infected chimpanzees. J. Virol. **71:**5769–5773.
24. **Shimizu, Y. K., A. Iwamoto, M. Hijikata, R. H. Purcell, and H. Yoshikura.** 1992. Evidence for in vitro replication of hepatitis C virus genome in a human T-cell line. Proc. Natl. Acad. Sci. USA **89:**5477–5481.
25. **Suh, Y. A., P. K. Kumar, K. Taira, and S. Nishikawa.** 1993. Self-cleavage activity of the genomic HDV ribozyme in the presence of various divalent metal ions. Nucleic Acids Res. **21:**3277–3280.
26. **Takeuchi, T., A. Katsume, T. Tanaka, A. Abe, K. Inoue, K. Tsukiyama-Kohara, R. Kawaguchi, S. Tanaka, and M. Kohara.** 1999. Real-time detection system for quantification of hepatitis C virus genome. Gastroenterology **116:**636–642.
27. **Tanaka, T., N. Kato, M. J. Cho, K. Sugiyama, and K. Shimotohno.** 1996. Structure of the 3′ terminus of the hepatitis C virus genome. J. Virol. **70:**3307–3312.
28. **Thomson, M., M. Nascimbeni, M. B. Havert, M. Major, S. Gonzales, H. Alter, S. M. Feinstone, K. K. Murthy, B. Rehermann, and T. J. Liang.** 2003. The clearance of hepatitis C virus infection in chimpanzees may not necessarily correlate with the appearance of acquired immunity. J. Virol. **77:**862–870.
29. **Tsukiyama-Kohara, K., N. Iizuka, M. Kohara, and A. Nomoto.** 1992. Internal ribosome entry site within hepatitis C virus RNA. J. Virol. **66:**1476–1483.
30. **Tsukiyama-Kohara, K., S. Tone, I. Maruyama, K. Inoue, A. Katsume, H. Nuriya, H. Ohmori, J. Ohkawa, K. Taira, Y. Hoshikawa, F. Shibasaki, M. Reth, Y. Minatogawa, and M. Kohara.** 2004. Activation of the CKI-CDK-Rb-E2F pathway in full genome hepatitis C virus-expressing cells. J. Biol. Chem. **279:**14531–14541.
31. **Walter, E., R. Keist, B. Niederost, I. Pult, and H. E. Blum.** 1996. Hepatitis B virus infection of tupaia hepatocytes in vitro and in vivo. Hepatology **24:**1–5.
32. **Wasley, A., and M. J. Alter.** 2000. Epidemiology of hepatitis C: geographic differences and temporal trends. Semin. Liver Dis. **20:**1–16.
33. **Xie, Z. C., J. I. Riezu-Boj, J. J. Lasarte, J. Guillen, J. H. Su, M. P. Civeira, and J. Prieto.** 1998. Transmission of hepatitis C virus infection to tree shrews. Virology **244:**513–520.
34. **Xu, X., H. Chen, X. Cao, and K. Ben.** 2007. Efficient infection of tree shrew (Tupaia belangeri) with hepatitis C virus grown in cell culture or from patient plasma. J. Gen. Virol. **88:**2504–2512.
35. **Yanagi, M., R. H. Purcell, S. U. Emerson, and J. Bukh.** 1997. Transcripts from a single full-length cDNA clone of hepatitis C virus are infectious when directly transfected into the liver of a chimpanzee. Proc. Natl. Acad. Sci. USA **94:**8738–8743.
36. **Yanagi, M., M. St Claire, M. Shapiro, S. U. Emerson, R. H. Purcell, and J. Bukh.** 1998. Transcripts of a chimeric cDNA clone of hepatitis C virus genotype 1b are infectious in vivo. Virology **244:**161–172.
37. **Zhao, X., Z. Y. Tang, B. Klumpp, G. Wolff-Vorbeck, H. Barth, S. Levy, F. von Weizsacker, H. E. Blum, and T. F. Baumert.** 2002. Primary hepatocytes of Tupaia belangeri as a potential model for hepatitis C virus infection. J. Clin. Invest. **109:**221–232.

THE JOURNAL OF BIOLOGICAL CHEMISTRY VOL. 284, NO. 52, pp. 36442–36452, December 25, 2009

Hepatitis C Virus Impairs p53 via Persistent Overexpression of 3β-Hydroxysterol Δ24-Reductase*[S]

Received for publication, July 10, 2009, and in revised form, October 24, 2009 Published, JBC Papers in Press, October 27, 2009, DOI 10.1074/jbc.M109.043232

Tomohiro Nishimura[‡§1], Michinori Kohara[¶1], Kosuke Izumi[‖], Yuri Kasama[‡], Yuichi Hirata[¶], Ying Huang[‖2], Masahiro Shuda[¶3], Chise Mukaidani[**], Takashi Takano[¶], Yuko Tokunaga[‡], Hideko Nuriya[¶], Masaaki Satoh[‡], Makoto Saito[‡], Chieko Kai[‖], and Kyoko Tsukiyama-Kohara[‡4]

From the [‡]Department of Experimental Phylaxiology, Faculty of Medical and Pharmaceutical Sciences, Kumamoto University, 1-1-1 Honjo, Kumamoto, Kumamoto 860-8556, the [§]Chemo-Sero-Therapeutic Research Institute, Kikuchi Research Center, Kyokushi, Kikuchi, Kumamoto 869-1298, the [¶]Department of Microbiology and Cell Biology, Tokyo Metropolitan Institute of Medical Science, 1-6 Kamikitazawa 2-chome, Setagaya-ku, Tokyo 156-8506, the [‖]Laboratory Animal Research Center, Institute of Medical Science, University of Tokyo, 4-6-1 Shirokane-dai, Minato-ku, Tokyo 108-8639, and the [**]Study Service Department, PhoenixBio Company, Ltd., 3-4-1 Kagamiyama, Higashi-Hiroshima 739-0046, Japan

Persistent infection with hepatitis C virus (HCV) induces tumorigenicity in hepatocytes. To gain insight into the mechanisms underlying this process, we generated monoclonal antibodies on a genome-wide scale against an HCV-expressing human hepatoblastoma-derived cell line, RzM6-LC, showing augmented tumorigenicity. We identified 3β-hydroxysterol Δ24-reductase (DHCR24) from this screen and showed that its expression reflected tumorigenicity. HCV induced the DHCR24 overexpression in human hepatocytes. Ectopic or HCV-induced DHCR24 overexpression resulted in resistance to oxidative stress-induced apoptosis and suppressed p53 activity. DHCR24 overexpression in these cells paralleled the increased interaction between p53 and MDM2 (also known as HDM2), a p53-specific E3 ubiquitin ligase, in the cytoplasm. Persistent DHCR24 overexpression did not alter the phosphorylation status of p53 but resulted in decreased acetylation of p53 at lysine residues 373 and 382 in the nucleus after treatment with hydrogen peroxide. Taken together, these results suggest that DHCR24 is elevated in response to HCV infection and inhibits the p53 stress response by stimulating the accumulation of the MDM2-p53 complex in the cytoplasm and by inhibiting the acetylation of p53 in the nucleus.

Hepatitis C virus (HCV)[5] is composed of a single-stranded RNA genome of positive polarity (1). Translation of viral proteins is initiated from an internal ribosome entry site (2) and results in a single polypeptide that is subsequently cleaved by host and viral proteases to yield viable proteins (3). The HCV genome does not rely on canonical translation factors and can readily establish chronic infection without integrating into the host genome, resulting in hepatic steatosis and hepatocellular carcinoma (HCC) (4). More than 170 million people worldwide are infected with HCV (5); chronic HCV infection and aging are the major risk factors for HCC (6–8). Liver cancer is the fifth most common cause of cancer mortality worldwide (9). The frequent inactivation of p53 in human HCC suggests that the loss of p53-dependent apoptosis may promote hepatocarcinogenesis (10). Chronic HCV infection results in chronic liver inflammation and induces endoplasmic reticulum stress and oxidative stress, which are thought to induce hepatocarcinogenesis (11, 12). The mechanistic details underlying HCC development are not fully understood. To gain insight into the molecular mechanisms underlying HCV-induced pathogenesis, we previously established RzM6 cells (13), a human hepatoblastoma (HepG2)-derived cell line in which expression of the full-length HCV genome is controlled by a Cre/*loxP* system. Expression of the HCV genome promoted anchorage-independent growth of RzM6 cells after 44 days of culture from the onset of HCV expression (RzM6-44d cells) but not in RzM6 cells after 0 days (RzM6-0d cells) (13). In the present study, we generated monoclonal antibodies against RzM6 cells cultured for longer than 44 days (RzM6-LC cells) and then screened the antibodies for their ability to bind antigens overexpressed in these cells. We identified 3β-hydroxysterol Δ24-reductase (DHCR24) from this screen and characterized its role in the HCV-induced cell growth deregulation.

EXPERIMENTAL PROCEDURES

Cells, Growth Assay, and Plasmids—HepG2 human hepatoblastoma cells, HuH-7 human hepatoma cells, WRL68 human embryonic hepatic cells, HEK293 human embryonic kidney cells, and human WI38 fibroblast cells were purchased from the American Type Culture Collection. NIH3T3 mouse fibroplast cells were from Japanese Collection of Research Bioresource. Cells were cultured under the growth conditions described in the supplemental material. RzM6 cells were established by

* This work was supported by grants from the Ministry of Health and Welfare of Japan, the Ministry of Education, Culture, Sports, Science and Technology of Japan, the Program for Promotion of Fundamental Studies in Health Sciences of the National Institute of Biomedical Innovation, the Cooperative Research Project on Clinical and Epidemiological Studies of Emerging and Re-emerging Infectious Diseases, and the Hayashi Memorial Foundation for Female Natural Scientists.

[S] The on-line version of this article (available at http://www.jbc.org) contains supplemental Figs. 1–5.

[1] Both authors contributed equally to this work.
[2] Present address: Liver Diseases Branch, NIDDK, National Institutes of Health, Bethesda, MD 20892.
[3] Present address: Molecular Virology Program, University of Pittsburgh Cancer Institute, University of Pittsburgh, 5117 Centre Ave., Pittsburgh, PA 15213.
[4] To whom correspondence should be addressed. Tel.: 81-96-373-5560; Fax: 81-96-373-5560; E-mail: kkohara@kumamoto-u.ac.jp.

[5] The abbreviations used are: HCV, hepatitis C virus; HCC, hepatocellular carcinoma; siRNA, small interfering RNA; HA, hemagglutinin; ELISA, enzyme-linked immunosorbent assay; HBV, hepatitis B virus.

transfection of HepG2 cells with the plasmid *HCR6*-Rz, which contains the full-length HCV cDNA (nucleotides 1–9611; GenBank™ accession number AY045702), and stably transformed cell lines were selected in media containing G418 (800 μg/ml bioactive; Invitrogen). These cell lines, termed 2–18, were then transfected with pCAG-Mer-Cre-Mer (Cre/*loxP* system) and were selected in media containing puromycin (Sigma), as described previously (13), to generate the RzM6 cell line. HCV expression was induced by treatment with 4-hydroxy-tamoxifen (100 nM). Cells expressing HCV for 44 days (RzM6-44d cells) displayed augmented anchorage-independent cell growth. Cells expressing HCV for more than 44 days are referred to as RzM6-LC cells.

The tumor formation assay was performed by injecting RzM6-0d, RzM6-44d, or RzM6-LC cells in the exponential growth phase into nude mice. Cells in culture were harvested with trypsin, and 2×10^6 or 1×10^7 cells were subcutaneously injected into the backs of athymic nude mice (ICR strain, Charles River). HepG2 and WRL68 cells with plasmid DNA or small interfering RNA (siRNA) were transiently transfected using Lipofectamine 2000 or RNAi Max (Invitrogen). HepG2 cells transfected with the pcDNA3.1-based HA- and FLAG-tagged DHCR24 expression vector were selected in media containing 800 μg/ml G418 (Invitrogen). The terminal deoxynucleotidyltransferase-mediated dUTP nick end labeling assay was performed using the TMR red *in situ* cell death detection kit (Roche Applied Science).

Generation of Monoclonal Antibodies—BALB/c mice received seven or eight intraperitoneal injections of RzM6-44d cells (5×10^6 cells/injection) in RIBI adjuvant (trehalose dimycolate + monophosphoryl lipid A emulsion; RIBI ImmunoChemResearch) at 3–4-week intervals. At the end of this immunization regimen, the spleens were removed, and the splenocytes were fused with mouse myeloma PAI cells using polyethylene glycol 1500 (Roche Applied Science), as described previously (14). Hybridoma cells were selected in medium containing hypoxanthine, aminopterin, and thymidine (Invitrogen), and culture supernatants were collected for whole-cell enzyme-linked immunosorbent assay (ELISA) screening.

ELISA, Immunostaining, Northern Blotting, Western Blotting, and Immunoprecipitation—Immunofluorescence assays, whole-cell ELISA, standard ELISA, and immunostaining are described in the supplemental materials. Northern blotting was performed as described previously (13). For immunoprecipitation and Western blotting, frozen specimens were homogenized on ice using a Dounce homogenizer fitted with a type-A pestle (Wheaton Science Products) in radioimmune precipitation buffer (1% SDS, 0.5% (v/v) Nonidet P-40, 0.15 M NaCl, 10 mM Tris, pH 7.4, 5 mM EDTA, and 1 mM dithiothreitol). Western blotting was performed as previously described (13) with the following primary antibodies: anti-DHCR24 monoclonal antibody 2-152a, polyclonal anti-p53 (Cell Signaling Technologies), anti-MDM2 (murine double minute clone 2 oncoprotein) (Santa Cruz Biotechnology, Inc., Santa Cruz, CA), anti-Myc (9E10) (Santa Cruz Biotechnology, Inc.), and anti-HCV core protein monoclonal antibody 515 (15) or 31-2. Anti-p53 monoclonal antibody (DO-1) and polyclonal antibody (FL-393) (Santa Cruz Biotechnology, Inc.) were used for immunostaining. Phosphorylation of p53 was characterized by Western blotting with antibodies against phosphorylated Ser^6, Ser^9, Ser^{15}, Ser^{20}, Ser^{37}, Ser^{46}, and Ser^{329} (Cell Signaling Technologies). Acetylation of p53 was examined by immunoprecipitation with anti-p53 (DO-1) and the ExactaCruz immunoprecipitation reagent (Santa Cruz Biotechnology, Inc.), followed by Western blotting with antibodies against p53 (rabbit polyclonal; Cell Signaling) or acetylated p53 (Lys^{373}/Lys^{382}) (Upstate Biotechnology). The interaction between p53 and MDM2 was examined by immunoprecipitation with anti-p53 (FL-393) or anti-MDM2 (H221; Santa Cruz Biotechnology, Inc.) and protein A-Sepharose (GE Healthcare), followed by Western blotting with monoclonal antibodies against MDM2 (SMP14, Santa Cruz Biotechnology, Inc.) and p53 (DO-1), respectively. Polyclonal anti-actin (Santa Cruz Biotechnology, Inc.), anti-histone H1 (Santa Cruz Biotechnology, Inc.), and anti-heat shock protein 70 (HSP70) (Stressgen) primary antibodies were used for normalization of Western blots. Subcellular fractionation of RzM6-0d and LC cells was performed as previously described (15).

Cloning and Expression of DHCR24 and in Vitro Translation—Total RNA was isolated from 1×10^6 HuH-7 cells using ISOGEN Reagent (Nippon Gene). Purified RNA (2 μg) was reverse-transcribed with Superscript II (Invitrogen) using random primers according to the manufacturer's protocol. The DHCR24 cDNA was then amplified by PCR with Phusion DNA polymerase (BioLabs). The following primers were used for the first round of amplification: D-5-1 (5′-CCCGGGCTGTGGGCTACAGG-3′, forward) and D-3-1 (5′-CCAGGCCACTTTTATTTAAA-3′, reverse). Primers for the second round of amplification were D-5-2 (5′-GTTCTCGAGCAGTGACAGGAGGCGCGAAC-3′, forward) and D-3-2 (5′-GTTCTCGAGTCCAGGCGGGCTCCAGCTCA-3′, reverse). The amplified DHCR24 cDNA was subcloned into the pGEM-T easy vector (Promega). *In vitro* translation was performed using TNT(R) reticulocyte lysate (Promega) and the Express Protein Labeling Mix (New England Nuclear) in the presence of either [^{35}S]Met/Cys or non-radioactive methionine. Amplified DHCR24 cDNA was digested with XhoI and subcloned into the pCAG-PURO vector (16) for transfection into WRL68 cells using Lipofectamine 2000. Amplified DHCR24 cDNA was also subcloned into the pcDNA3.1 vector containing an HA or FLAG tag (kindly supplied by Dr. N. Takahashi, Tokyo University of Agriculture and Technology) for transfection into RzM6 or HepG2 cells using Lipofectamine LTX (Invitrogen). Transfected cells were selected in media containing G418.

The lentiviral vector, pCSII-EF-MCS-EMCV IRES-GFP (generous gift from Hiroyuki Miyoshi, RIKEN, Tsukuba, Japan), was modified by replacing the green fluorescent protein gene with the hygromycin phosphotransferase gene to construct pCSII-EF-MCS-EMCV IRES-Hygro. DHCR24 fused to the 5′-HA or 5′-FLAG tag-encoding sequence were cloned under the EF promoter. The resulting plasmid was cotransfected with packaging plasmid (pCAG-HIVgp and pCMV-VSVG-RSV-Rev) in 293FT cells (Invitrogen) to produce recombinant lentivirus. Following infection, cells were selected with hygromycin B (600 μg/ml; Sigma).

Silencing of DHCR24 and HCV by siRNA—The DHCR24 stealth siRNA was designed to target the human DHCR24 mRNA sequence 5′-GCAAGCUGAAUAGCAUUGGCAAUUA-3′ (nucleotides 970–993) using the BLOCK-iT RNAi designer (Invitrogen). A mutated siRNA (5′-GCAGUCUAACGAUUACGGAAAGUUA-3′) was synthesized as a control. An alternative siRNA, siDHCR24-1024, was designed as 5′-GAGAACUAUCUGAAGACAATT-3′. The HCV siRNA was synthesized as previously described (17). Cells were transfected with a 1 nM concentration of the chemically synthesized siRNAs using Lipofectamine 2000 or Lipofectamine RNAiMAX (Invitrogen) in Opti-MEM (Invitrogen) and then incubated for 4–6 h at 37 °C. Cells were characterized 48 h after transfection.

Caspase and Reporter Assays—Cells (1×10^4 cells/well) were seeded into white 96-well plates (Sumitomo Bakelite), treated with 1 mM H_2O_2, and then lysed with caspase-Glo 3/7 buffer (Promega). Caspase 3/7 activity was determined by measuring the absorbance resulting from cleavage of a proluminescent substrate containing the sequence DEVD (Promega) using a multilabel counter (PerkinElmer Life Sciences). The $p21^{WAF1/CIP1}$ promoter activity was assayed in HepG2, RzM6-0d, or RzM6-LC cells transfected with pWWP-Luc (kindly supplied by Dr. Bert Vogelstein (The Johns Hopkins University)). Cells were cotransfected with phRL-TK(Int-) (Promega) for normalization of promoter activity. Cells were incubated for 2 days after transfection and were then treated with 1 mM H_2O_2 for 4 h. Promoter activity was measured using the Dual-Luciferase reporter assay system (Promega).

HCV Infection of Humanized Chimeric Mouse Liver and mRNA Quantification by Quantitative Reverse Transcription-PCR—Detailed procedures are described in the supplemental material.

Statistical Analysis—Student's *t* test was used to test the statistical significance of the results. *p* values less than 0.05 were considered statistically significant.

RESULTS

Expression of DHCR24 Parallels Hepatocarcinogenesis—RzM6 cells expressing full-length HCV were established using the Cre/*loxP* expression-switching system (13). RzM6 cells cultured for longer than 44 days (termed RzM6-LC) had a greater ability to form colonies (13) and to induce tumors in nude mice (Fig. 1*A*). We produced monoclonal antibodies against RzM6-LC cells (see supplemental materials) and screened them for their ability to bind RzM6 antigens overexpressed upon the onset of hepatocarcinogenesis. Antibody clone 2-152a bound to a ~60-kDa protein (p60) that was expressed at higher levels in RzM6-LC cells than in RzM6 cells before the onset of HCV expression (termed RzM6-0d) (13) (Fig. 1*B*). p60 was strongly expressed in hepatoma-derived HuH-7 cells but was less abundant in the less aggressive cancer cell line, HepG2, or in the normal embryonic cell lines WRL68, HEK293, or NIH3T3 (supplemental Fig. 1*A*). To identify p60, the protein was purified from RzM6-LC cells using immunoaffinity chromatography and subjected to matrix-assisted laser desorption/ionization time-of-flight mass spectrometry (supplemental Fig. 1*B*). Through this process, p60 was identified as DHCR24 (also known as seladin-1) (18–20), an enzyme that catalyzes the reduction of the Δ-24 double bond of sterol intermediates during cholesterol biosynthesis and is up-regulated by oxidative stress (19, 21). DHCR24 cDNA was cloned and translated *in vitro* (Fig. 1*C*) and also expressed in human embryonic hepatic WRL68 cells (Fig. 1*D*), and the monoclonal antibody 2-152a reacted with the expressed protein (Fig. 1, *D* and *E*).

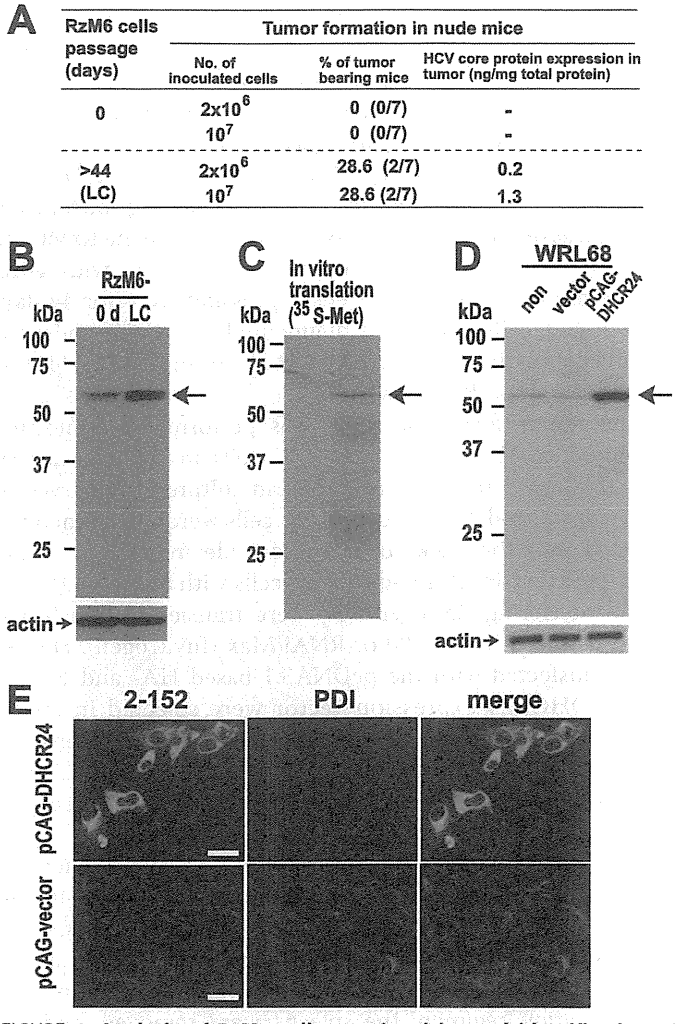

FIGURE 1. **Analysis of RzM6 cell tumorigenicity and identification of DHCR24 overexpression in RzM6-LC cells.** *A*, summary of tumor formation in nude mice injected with RzM6-0d or RzM6-LC cells. *B*, detection of a ~60-kDa protein (*arrow, upper panel*) in whole-cell lysates (30 μg/lane) from RzM6-0d and RzM6-LC cells by Western blotting with monoclonal antibody 2-152a. Anti-actin antibody was used for normalization (*arrow, lower panel*). Data are representative of two independent experiments. *C*, empty vector (pGEM3, *left lane*) or pGEM-DHCR24 (*right lane*) was subjected to *in vitro* transcription/translation using rabbit reticulocyte lysates in the presence of [^{35}S]methionine. Samples were subjected to SDS-PAGE followed by autoradiography. *D*, cell lysates from untransfected WRL68 cells (*non*), WRL68 cells transfected with empty pCAG vector (*vector*), and WRL68 cells transfected with pCAG-DHCR24 vector were examined by Western blotting with monoclonal antibody 2-152a (*upper panel*) or monoclonal anti-actin antibody (*lower panel*). *E*, WRL68 cells were transfected with pCAG-DHCR24 or pCAG vector alone and subjected to immunocytochemistry with monoclonal antibody 2-152a (*green*) or anti-protein-disulfide isomerase antibody (*PDI*; *red*). *Scale bars*, 25 nm.

HCV Induces Persistent DHCR24 Overexpression—Since DHCR24 was up-regulated in RzM6-LC cells, we examined whether HCV can induce DHCR24 expression in human hepatocytes. We also compared the expression levels of DHCR24

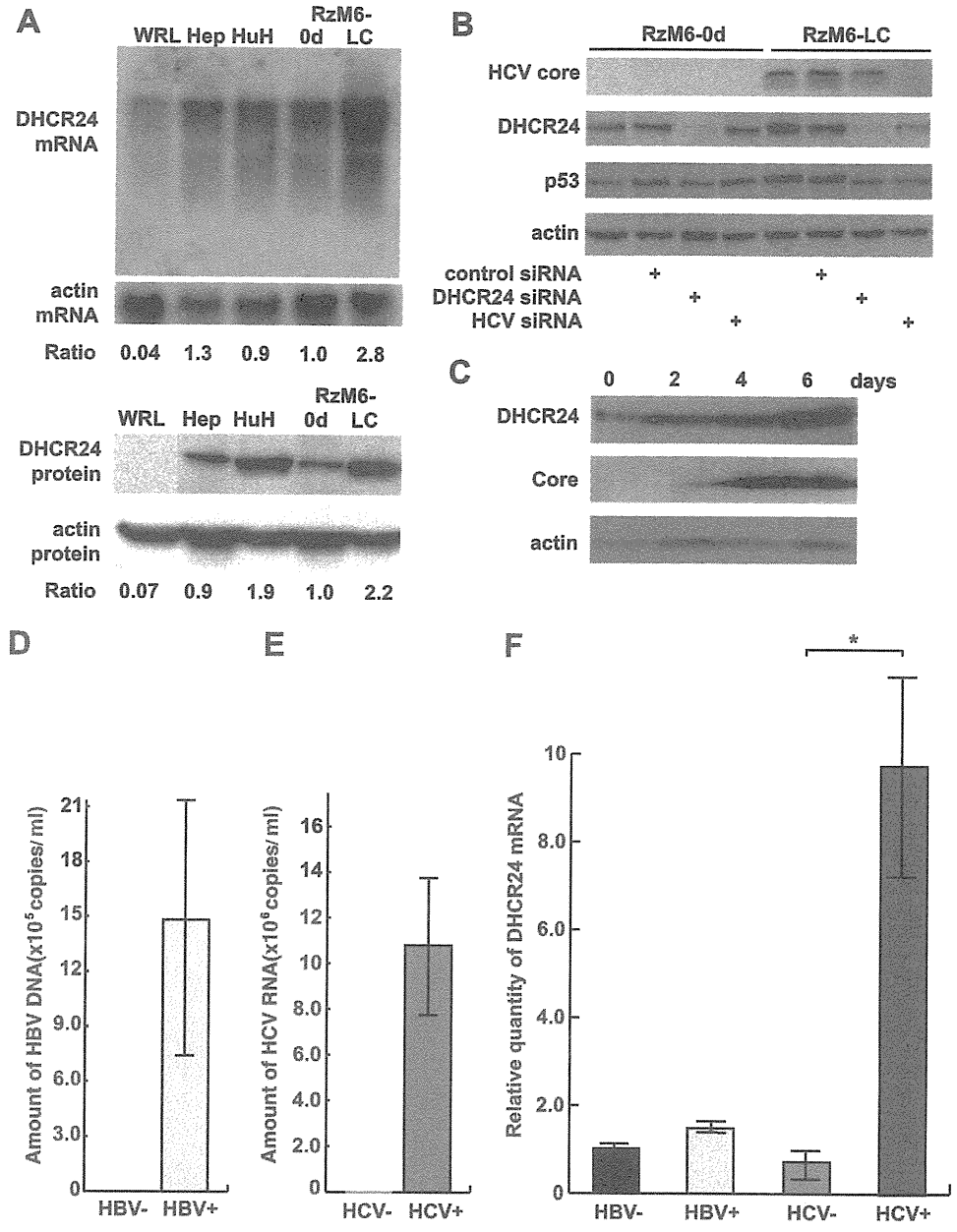

FIGURE 2. **Induction of DHCR24 by HCV in human liver cell lines.** *A*, expression of DHCR24 mRNA (Northern blot, *upper panel*) and protein (Western blot, *lower panel*) in WRL68 (*WRL*), HepG2 (*Hep*), HuH-7 (*HuH*), RzM6-0d, and RzM6-LC cells. Ratios indicate the amount of DHCR24 mRNA or protein in each cell type (quantified by densitometry) relative to that of RzM6-0d cells. *B*, Western blotting of HCV core protein, DHCR24, and p53 (DO-1 antibody) proteins in RzM6-0d and RzM6-LC cells following treatment with the indicated (+) siRNA. *C*, the induction of DHCR24 by HCV after 2, 4, and 6 days in RzM6 cells by treatment of tamoxifen (100 nM). Data are representative of two independent experiments, and anti-actin antibody was used as a loading control (*A–C*). *D*, amount of HBV DNA in HBV-infected human hepatocytes in chimeric mouse liver quantitated by RTD-PCR. *E*, amount of HCV-RNA in HCV-infected human hepatocytes in chimeric mouse liver quantitated by RTD-PCR. *F*, the quantitation of DHCR24 mRNA in mock-infected, HBV-infected, and HCV-infected human hepatocytes in chimeric mouse liver. *Vertical bars*, S.D.; *, $p < 0.05$ (two-tailed Student's *t* test).

protein and mRNA in a panel of hepatic and embryonic cell lines (Fig. 2*A*). Northern blotting revealed that DHCR24 mRNA expression was notably higher in RzM6-LC cells than in RzM6-0d cells, indicating that induction of DHCR24 occurs at the transcriptional level. DHCR24 protein levels were also higher in HuH-7 and RzM6-LC cells relative to RzM6-0d cells (Fig. 2*A*). To examine whether persistent up-regulation of *DHCR24* in RzM6-LC cells resulted from HCV expression, we utilized an siRNA to knockdown HCV expression (17) (Fig. 2*B*). Silencing HCV by greater than 99% with siRNA reduced the expression of DHCR24 and p53 in RzM6-LC cells. When we induced HCV expression with tamoxifen, the induction of DHCR24 was observed after 2, 4, and 6 days (Fig. 2*C*). These results indicate that expression of the full-length HCV genome induced DHCR24 overexpression. DHCR24 was not induced in HuH-7 cells infected with the HCV strain JFH-1 (22) (data not shown). This result might be explained by the substantial endogenous expression of DHCR24 in HuH-7 cells (Fig. 2*A* and supplemental Fig. 1*A*). To examine whether HCV infection can induce DHCR24, human hepatocytes in chimeric mice were infected with hepatitis B virus (HBV) or HCV (Fig. 2, *D* and *E*). Notable up-regulation of DHCR24 mRNA was detected in HCV-infected human hepatocytes but not in HBV-infected human hepatocytes (Fig. 2*F*).

Persistent Overexpression of DHCR24 Induces Apoptotic Resistance to Oxidative Stress—As HCV infection increased the expression of DHCR24, we further examined the effect of DHCR24 on hepatocytes. Because DHCR24 regulates oxidative stress-induced apoptosis (19, 21, 23, 24), the terminal deoxynucleotidyltransferase-mediated dUTP nick end labeling assay was performed with RzM6 cells to examine the effect of DHCR24 overexpression on H_2O_2-induced apoptosis (Fig. 3*A*). Fragmentation of genomic DNA was less pronounced in DHCR24-overexpressing cells (RzM6-LC cells and RzM6-0d cells transduced with DHCR24 lentivirus) than in RzM6-0d cells or RzM6-0d cells transduced with empty lentiviral vector. To quantify the apoptotic response, we examined the effect of DHCR24 overexpression on caspase activity (Fig. 3, *B–D*). Caspase activation by H_2O_2 was suppressed in RzM6-LC cells compared with RzM6-0d cells (Fig. 3*B*). Transfection with HCV siRNA recovered the caspase response in RzM6-LC cells. Caspase 3/7 activity was also examined following the transfection of HepG2 cells with pCA-Rz (Fig. 3*C*). Induction of caspase activation by H_2O_2 was inhibited by expression of the HCV gene; the inhibition was partially recovered by transfection with DHCR24

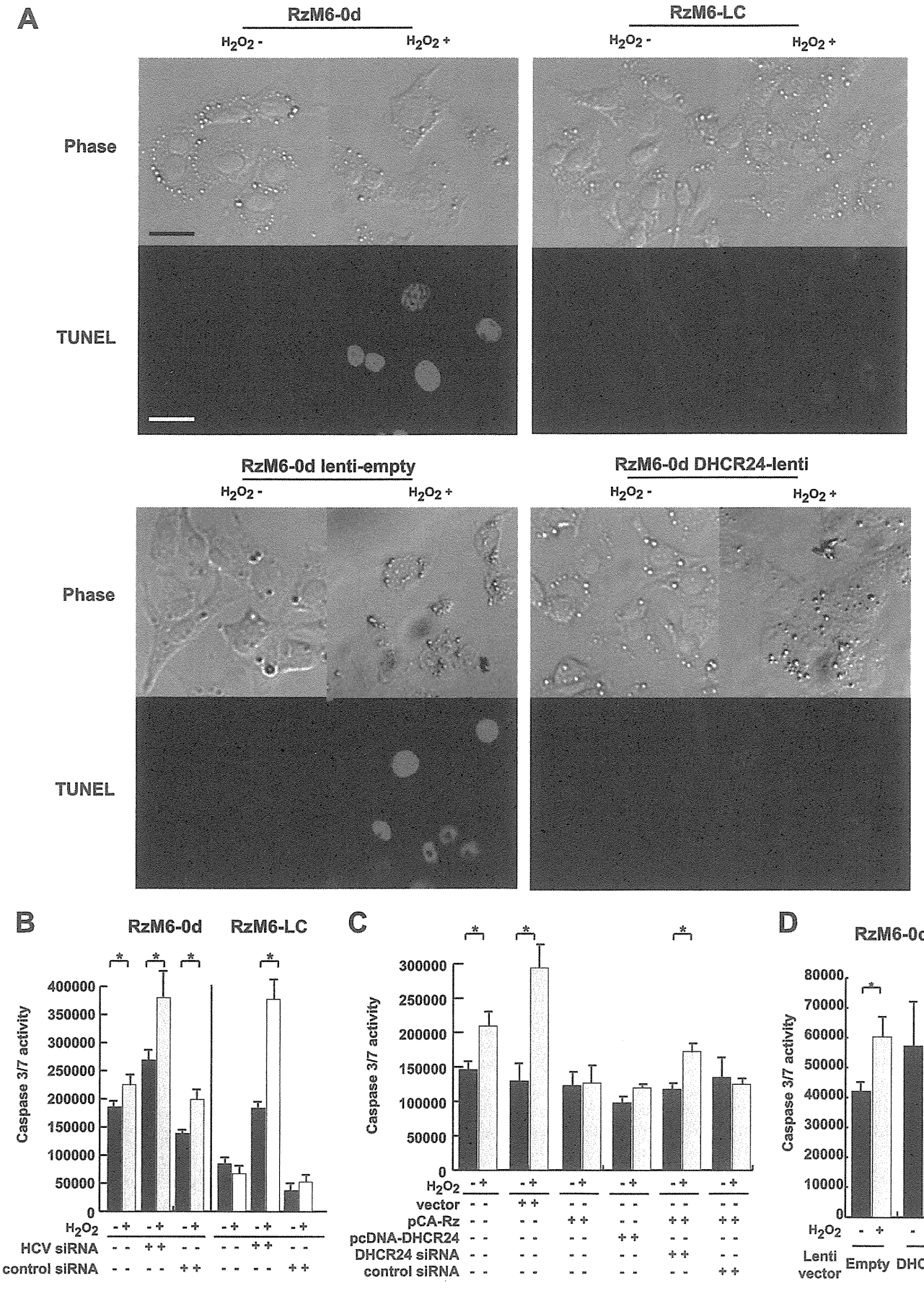

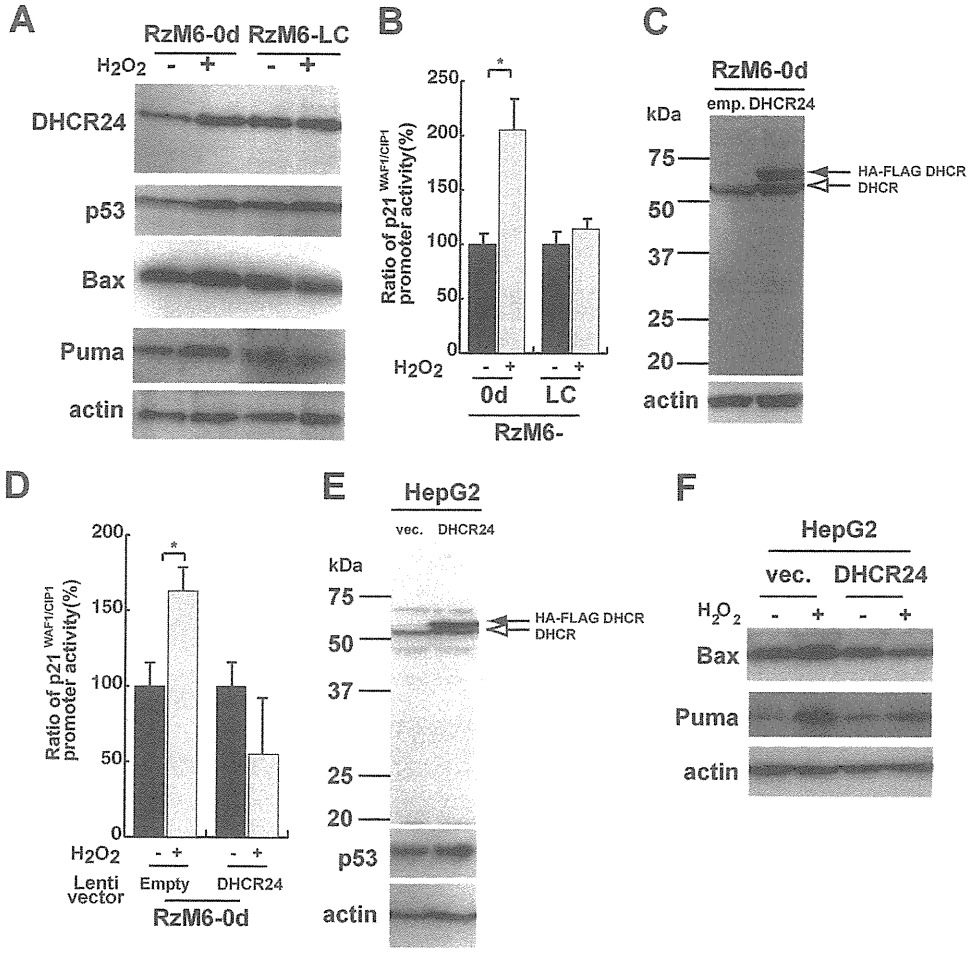

FIGURE 4. **Persistent overexpression of DHCR24 impairs p53 activity.** *A*, Western blotting of RzM6-0d and RzM6-LC cells treated with or without H_2O_2 was performed using antibodies against the proteins indicated on the *left*. *B*, $p21^{WAF1/CIP1}$ promoter activity in RzM6-0d and RzM6-LC cells transfected with pWWP-Luc followed by treatment with or without H_2O_2. Promoter activity was calculated as the ratio of firefly luciferase activity to *Renilla* luciferase activity. The ratio of promoter activity with H_2O_2 treatment to without H_2O_2 treatment is indicated as a percentage. *C*, DHCR24 expression in RzM6-0d cells transduced with lenti-empty (*emp.*) or lenti-DHCR24 (with HA-FLAG tag) vector. *D*, $p21^{WAF1/CIP1}$ promoter activity in RzM6-0d cells transfected with lenti-empty or lenti-DHCR24 vector followed by treatment with or without H_2O_2. Promoter activity was calculated as the ratio of firefly luciferase activity to *Renilla* luciferase activity. The ratio of promoter activity with H_2O_2 treatment to activity without H_2O_2 treatment is indicated as a percentage. *E*, HepG2 cells transfected with pcDNA vector (*vec*) or DHCR24 expression vector (pcDNA-DHCR24 HA-FLAG tag; *DHCR24*) and selected by G418 were analyzed by Western blotting with DHCR24 monoclonal antibody 2-152a (*top*), p53 monoclonal antibody (DO-1) (*middle*), and actin (*bottom*). *F*, expression of Bax and Puma in HepG2 cells transfected with pcDNA vector (*vec*) or pcDNA-DHCR24 vector followed by treatment with or without H_2O_2 was analyzed by Western blotting with antibodies to the proteins indicated at the *left*. Actin was analyzed as a control. In *A–F*, representative data from three independent experiments are shown; *, $p < 0.05$ (two-tailed Student's *t* test).

siRNA. Moreover, overexpression of DHCR24 from a lentivirus vector (Fig. 3*D*) (25) or from transfection with a DHCR24 expression vector (data not shown) impaired H_2O_2-induced caspase activation in RzM6-0d cells. Thus, enhanced expression of DHCR24 promotes resistance to H_2O_2-induced apoptotic responses, and HCV-induced apoptotic resistance is partially mediated by DHCR24.

Persistent Overexpression of DHCR24 Inhibits p53 Activity—H_2O_2 induces p53-dependent apoptosis (26). Expression of the p53-induced apoptotic response mediators, Bax (27) and Puma (28), did not increase after H_2O_2 treatment of RzM6-LC cells (Fig. 4*A*). Therefore, we examined p53 expression and function in DHCR24-overexpressing cells. H_2O_2 increased the expression of DHCR24 and p53 in RzM6-0d cells. By comparison, the expression of these proteins was already elevated prior to H_2O_2 treatment in RzM6-LC cells, and we found no further H_2O_2-induced increase in expression (Fig. 4*A*). Consistent with these findings, H_2O_2 activated transcription from the $p21^{WAF1/CIP}$ promoter in RzM6-0d cells but not in RzM6-LC cells (Fig. 4*B*). This response of the $p21^{WAF1/CIP}$ promoter is impaired in cells overexpressing DHCR24 via the lentivirus vector (Fig. 4, *C* and *D*) or via the expression vector (Fig. 4*E*). Induction of Bax and Puma expression after H_2O_2 treatment was decreased in DHCR24-overexpressing cells (Fig. 4*F*). These results indicate that although p53 expression is elevated in DHCR24-overexpressing cells, the function of p53 in the oxidative stress pathway is impaired.

Overexpression of DHCR24 Enhances the Interaction between p53 and MDM2—Since DHCR24 is a regulator of the p53-MDM2 interaction (21), we examined the interaction between p53 and its specific ubiquitin ligase, MDM2. Unexpectedly, the interaction between p53 and MDM2 was stronger in RzM6-LC cells than in RzM6-0d cells (Fig. 5, *A* and *B*). Lentiviral vector overexpression of DHCR24 in RzM6-0d cells increased the binding of p53 to MDM2 (data not shown). Furthermore, cell fractionation analysis revealed that the interaction between MDM2 and p53 mostly occurred in the cytoplasmic fraction, even after H_2O_2

FIGURE 3. **Prior overexpression of DHCR24 inhibits H_2O_2-induced apoptosis.** *A*, representative phase-contrast images of RzM6-0d and RzM6-LC cells (*upper panels*) or lenti-empty and lenti-DHCR24 vector-transduced RzM6-0d cells (*lower panels*) treated with or without H_2O_2 (1 mM, 4 h). *In situ* cell death was detected by the terminal deoxynucleotidyltransferase-mediated dUTP nick end labeling (*TUNEL*) assay with tetramethylrhodamine. *Scale bars*, 25 nm. Representative data from three experiments are shown. *B*, caspase 3/7 activity (relative light units) in RzM6-0d and RzM6-LC cells treated with or without H_2O_2. Cells were transfected with or without HCV siRNA or with control siRNA as indicated. *C*, caspase 3/7 activity in HepG2 cells treated with or without H_2O_2. Cells were transfected with control pcDNA vector (vector), pCA-Rz, pcDNA-DHCR24, DHCR24 siRNA, or control siRNA. *D*, caspase 3/7 activity in RzM6-0d cells treated with or without H_2O_2. Cells were transduced with lenti-empty or lenti-DHCR24 vector. In *B–D*, data reflect the means ± S.D. of three independent triplicate experiments; *, $p < 0.05$ (two-tailed Student's *t* test).

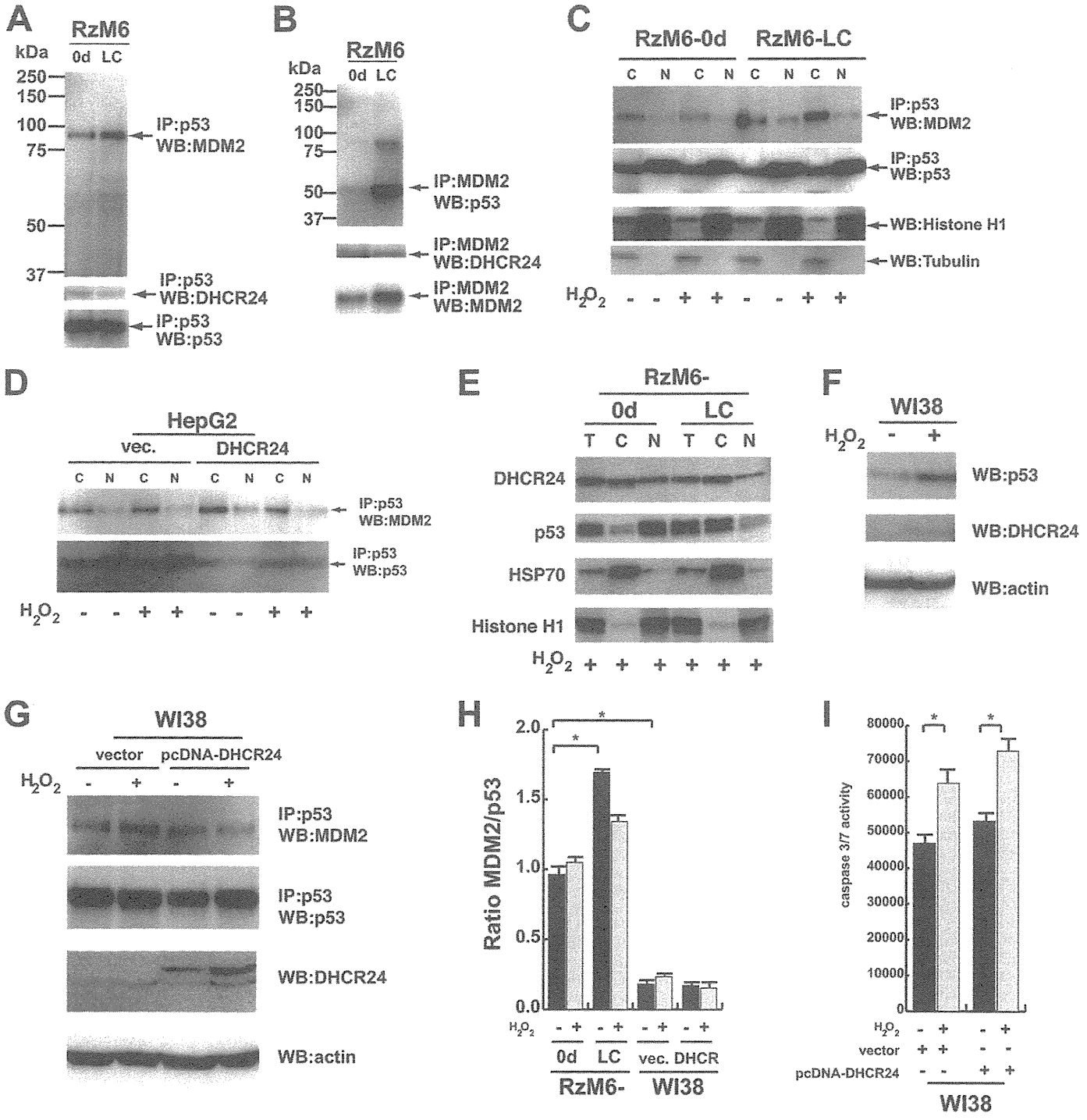

FIGURE 5. **DHCR24 overexpression enhances the interaction between p53 and MDM2 in the cytoplasm.** *A*, p53 was immunoprecipitated (*IP*) from RzM6-0d and RzM6-LC cells with polyclonal anti-p53 antibody (FL393) followed by Western blotting with monoclonal antibodies against MDM2 (*top*) and p53 or DHCR24 (*bottom*). *B*, MDM2 was immunoprecipitated from RzM6-0d and RzM6-LC cells using polyclonal anti-MDM2 antibody (H221) followed by Western blotting (*WB*) with monoclonal antibodies against p53 (*top*) and MDM2 or DHCR24 (*bottom*). *C*, p53 was immunoprecipitated from cytoplasmic (*C*) or nuclear (*N*) fractions of RzM6-0d and LC cells using anti-p53 antibody (FL393) followed by Western blotting with anti-MDM2 antibody (*top*) and anti-p53 antibody (*bottom*). Cell fractionation was confirmed by Western blotting with anti-histone H1 and tubulin (*WB*). *D*, p53 was immunoprecipitated from cytoplasmic or nuclear fractions of HepG2 cells transfected with control pcDNA (*vec*) or pcDNA-DHCR24 expression vector using polyclonal anti-p53 (FL393) followed by Western blotting with antibodies against the proteins indicated at the right. Reaction with secondary antibodies (anti-rabbit or mouse IgG conjugated with horseradish peroxidase) alone did not show any signal (data not shown), and data representative of three independent experiments are shown (*A–D* and *G*). *E*, RzM6-0d or RzM6-LC cells with H_2O_2 treatment were fractionated into total (*T*), cytoplasmic, and nuclear fractions and subjected to Western blotting with the antibodies indicated on the *left*. *F*, Western blotting of WI38 cells with or without H_2O_2 treatment (0.5 mM, 4 h) with antibodies against p53, DHCR24, and actin. *G*, immunoprecipitation of p53 from cells transfected with pcDNA vector and pcDNA-DHCR24 (*DHCR*) with or without H_2O_2 treatment (0.5 mM, 4 h), followed by Western blotting with antibodies against MDM2 (*first column*) and p53 (*second column*). Cells were examined with Western blotting with anti-DHCR24 (*third column*) and anti-actin (*fourth column*). *H*, the average ratio of the quantified results of immunoprecipitation of p53 and Western blotting of MDM2 in RzM6-0d, RzM6-LC, and WI38 cells with transfection of pcDNA vector or pcDNA-DHCR24 with or without H_2O_2 treatment are indicated. *Vertical bars*, S.D. *, $p < 0.05$ (two-tailed Student's *t* test). *I*, a caspase 3/7 assay was performed in WI38 cells with pcDNAvector (vector) and pcDNA-DHCR24 overexpression vector. *Vertical bars*, S.D. *, $p < 0.05$ (two-tailed Student's *t* test).